Alignment of Image Sensor Using Piezoelectric Crystals

Reem Chahrour & Julia Jakobsson

2023

Master´s Thesis in
Electrical Measurements

In collaboration with Axis Communications AB

Company supervisor: Peter Lehtinen
Academic supervisor: Lars Wallman

LUND
UNIVERSITY

Faculty of Engineering LTH
Department of Biomedical Engineering

"How to Achieve Crystal Clear Focus: "

Reem & Julia

LUND UNIVERSITY

Abstract

Alignment of Image Sensor Using Piezoelectric Crystals

by Reem Chahrour & Julia Jakobsson

The use of piezoelectric crystals as a way to achieve automatic alignment of an image sensor in a camera was investigated in collaboration with Axis Communications AB. Piezoelectric crystals can be created into different configurations, piezoelectric stacks being one of the simpler ones. By attaching three piezoelectric stacks behind an image sensor and applying voltage to the stacks, they expand and the length between the sensor and the lens component is altered thus a change in the amount of focus will occur.

Tests conducted in both a light controlled environment provided by Axis as well as in scenes similar to those of a user, showed promising results of focus correction with the use of a lens displacement of 41 μm. Furthermore, the unique quality of tilting of the image sensor was investigated. An auto focus algorithm was used to automatically align the center and corners of the image. Moreover, deliberate tilting was employed to adjust the focus placement in the image. Findings suggest that piezoelectric crystals are an effective method for achieving automatic alignment and controllable focus in cameras, with promising results in both controlled and real-world environments.

Overall, this study demonstrates the potential of using piezoelectric crystals for automatic alignment and controllable tilt in cameras. Although further investigations are needed before the solution can be used in a product, our findings provide a foundation for future research in this area.

Sammanfattning

I denna rapport undersöktes användningen av piezoelektriska kristaller som ett sätt att uppnå automatisk justering av en bildsensor i förhållande till en lins i en kamera; Detta gjordes i samarbete med Axis Communications AB. Det finns flera olika komponenter som använder sig av piezoelektriska kristaller, en av de enklare är piezoelektriska stackar. Genom att placera tre stackar bakom en bildsensor och applicera spänning på dessa expanderar de, vilket ändrar avståndet mellan sensorn och linskomponenten. Detta resulterar i en förändring av fokusvärdet.

Det utfördes tester både i en ljuskontrollerad miljö som tillhandahölls av Axis och i scenarier liknande verkliga användningsfall. Resultaten påvisade en ändring av fokus med hjälp av en expansion av de piezoelektriska stackarna på 41 μm. Dessutom undersöktes möjligheten att justera lutningen av bildsensorn. En autofokusalgoritm skapades och användes för att justera bildsensorns centrum och hörn, för att uppnå bästa möjliga fokus. Vidare användes "avsiktlig" lutning av sensor kortet för att justera fokusplanet i bilden. Resultaten tyder på att piezoelektriska stackar är en effektiv metod för att uppnå automatisk justering och kontrollerbar fokus i kameror.

Sammanfattningsvis demonstrerar och diskuterar denna rapport användningen av piezoelektriska kristaller för automatisk justering och kontrollerbar lutning av bildsensorn i kameror. Ytterligare undersökningar krävs innan denna teknologi kan implementeras i en produkt, men resultaten möjliggör en grund för framtida forskning och utvecklig inom detta område.

Acknowledgements

This thesis was conducted as a collaboration between Axis Communications AB and the Faculty of Engineering at Lund University from the 16th of January until the 30th of May 2023.

First of all, we would like to convey our sincerest appreciation to Peter Lehtinen and Maria Romedahl for believing in our ability to take on this project. Special thanks to Peter for guiding us and connecting us to the he right people during this process.

We express our deepest gratitude to Niklas Ekstrand for dedicating time to assist us with creating all the CAD models of the prototype. Furthermore, we are thankful for his support and guidance throughout the process, serving as a trusted advisor to us.

We would like to extend our utmost appreciation to Marko Stozinic (and MCP :)) for the assistance and guidance in all matters related to electronics. We are deeply grateful for the willingness to lend a helping hand. You're the boss!

A heartfelt thanks to Jenny Karlsson for always setting aside time to answer our questions regarding all things related to focus and providing valuable insights on conducting tests. Her willingness to share her knowledge and expertise has been instrumental in enhancing our understanding.

We extend our thanks to Fritjof Jonsson for his guidance throughout the process of writing the programming scripts, developing focus algorithms, and deciphering the code provided by Thorlabs.

We wish to convey our appreciation to Philip Stjärneblad for taking the time to help us set up the HIT test.

Thanks to Fredrik Österberg for sharing his knowledge about the cameras utilized in this project.

Special thanks to Lars Wallman for being our academic supervisor and Johan Nilsson for being our examiner.

We would like to extend our utmost thanks to our wonderful friends. Your unwavering friendship have brought us joy and laughter during both the highs and lows.

Julia: The first person I would like to thank is Reem. I have had a wonderful time doing this master's thesis with you. You are such a sweet and bright person. I wish you all the best in life!

I want to thank my family for always being my biggest cheerleaders. I would not have come this far without your support, it means the world. And a special thanks to my grandpa for the all the academical help and inspiration.

Lastly, I want to thank my Jacob, for all the support you have shown me during these five years. You make me a better person.

Reem: Of course, thanks to Julia, who has been the best thesis partner I could ever hope for. You are one of the smartest and kindest people I know.

I would like to thank my family, and especially my mom and dad for providing me with all the tools to make these last five years happen. Without your encouragements and support I would not be where I am today.

Last but certainly not least, I would like to thank my husband, Ali, for being my rock through it all. I am truly and forever grateful to have you by my side.

Contents

Abstract **v**

Sammanfattning **vii**

Acknowledgements **ix**

1 Introduction **1**
1.1 Background 1
1.2 Goals 2

2 Theory **3**
2.1 The Piezoelectric Effect 3
2.1.1 Crystal Structure 3
Lead Zirconate Titanate 4
2.1.2 The Piezoelectric Actuator 5
2.2 The Functionalities of a Camera 5
2.2.1 The Lens 6
F-number 6
Barrel Distortion 6
2.2.2 The Image Sensor 7
2.3 Focus Measurements 8
2.3.1 The Laplacian Operator and its Variance 8
2.3.2 The Modulation Transfer Function 9
Spatial Frequency Response 11
2.4 Electrical Properties 12

3 Market Analysis **15**
3.1 Requirements 15
3.2 Types of Piezoelectric Devices 15

4 Materials **19**
4.1 Discrete Piezoelectric Stacks 19
4.1.1 Hysteresis and Individual Properties 20
4.2 The Cameras 22
4.2.1 M3065 & M3085 22
4.2.2 M3088 22
4.2.3 Other equipment 23

5 Methodology **25**
5.1 Connecting the Piezoelectric Stacks 25
5.2 Siemens Stars 27
5.3 Characterization of the Prototype using HIT-Corner Focus Test and a Manual Stage 29
5.4 Real Life Environments 33
5.4.1 Through a Window 33
5.4.2 Along a Hallway 33
5.5 The Algorithm 33
5.6 Electrical Measurements 34

6 Prototype set-up **35**
6.1 The Prototype 35
6.1.1 Idea and Requirements 35
6.1.2 Early stages 36
6.2 Prototype 1 39
6.2.1 Change of Camera 42
6.3 Prototype 2 43
6.4 Tilt 46

7 Auto Focus Algorithm **51**
7.1 Background 51
7.2 The Algorithm 51
7.2.1 Structure of the Code 52
7.2.2 The Algorithm in Words 52
7.2.3 The Focus Value 53

8 Results & Discussion **55**
8.1 HIT Corner Focus-Measurements 55
8.1.1 M3085/65 - Manual 55

8.1.2 M3085/65 - Prototype 58
8.1.3 M3088 - Manual 59
8.1.4 M3088 - Prototype 60
8.2 Image Comparisons 60
8.2.1 M3065/85 - Prototype 60
8.2.2 Comparisons with the Manual set-up 63
M3085/65 - Manual Test 1 63
M3085/65 - Manual Test 2 65
M3088 - Manual Window Test 67
M3088 - Prototype Window Test 68
8.2.3 Close and Far Distances within the Same Image - Hallway 70
A Person at Different Distances 72
8.3 Focus algorithm 74
8.3.1 Hysteresis 75
8.3.2 Running the Algorithm 76
8.3.3 Automatic alignment 83
8.3.4 Deliberate tilting 87
8.4 Electrical Measurements 89
8.4.1 Power Consumption 89

9 Conclusion & Future Directions **93**
9.1 The Prototype and The (In)ability to Tilt 93
9.2 The Cameras 94
9.3 The Algorithm 94
9.4 Lead Free Piezoelectric Crystals 95
9.5 The Type Of Piezoelectric Device 96
9.6 Power Consumption 96
9.7 Products in Need of This Technology 97

A Auto Focus Algorithm **99**
.1 Class Camera 99
.2 Class Device 102
.3 Main 104

List of Figures

2.1 Perovskite crystal structure of PZT. Structure one is the lattice at 0V, and structure two is the lattice with an applied voltage. 4
2.2 This is how an image gets distorted by barrel distortion. 7
2.3 An example of a Bayer filter 8
2.4 a) An example of a common pattern used as a target for testing performance of optical systems. b) The brightness of the target. 1/N indicates the number of stripes per millimeter. 9
2.5 The spread function creates a blurred effect across edges. 9
2.6 When the test pattern (square wave) becomes smaller, the contrast in the image (sine wave) becomes smaller. 10
2.7 a) The system A and B has the same limiting resolution but A will produce a better image at low frequencies. b) System A will produce a better image at low frequencies but system B has a higher limiting resolution. The most suitable system must be based on the application. 11
2.8 Wiring diagram of the resistors and a capacitance. . . . 12

3.1 Amplified piezoelectric actuators from Thorlabs. The size is 14.0 x 7.0 x 44.0 mm [25]. 16
3.2 The piezoelectric stack used from Thorlabs [26]. 17

4.1 Schematic of the stacks used from Thorlabs. 20
4.2 Figure showing the displacement vs the voltage. Note the 15% hysteresis [26]. 21
4.3 The Axis M3088 Dome camera [5]. 23
4.4 The Thorlabs KPZ101 - K-Cube Piezo Controller [23]. Note that three of these was used. 24

4.5 The Thorlabs KCH301 Power Supply for Three K-Cubes [22]. 24

5.1 Wiring diagram of the resistors and piezoelectric stack. 26
5.2 The two resistors attached on to an SMA cable before soldered onto a piezoelectric stack. 26
5.3 Siemens star that was placed in some of the images [29]. 27
5.4 The usage of Siemens stars in a manual tests to make it easier for the naked eye to distinguish differences in focus. Note the blob in the middle of the Siemens stars indicating bad focus. 28
5.5 The defined ROI's are outlined in green and are used for the testing of the focus algorithm. 28
5.6 Thorlabs manual stage with a camera attached. 29
5.7 CAD illustration of the parts that fit into the manual stage from Thorlabs. Figure a) is for the M3085/65 camera, and b) is for the M3088 camera. 30
5.8 The target used in the HIT tests. 31
5.9 The HIT test set-up using the manual stage. 32
5.10 The HIT test set-up using the prototype. 32

6.1 First sketch ever made of the prototype. Note the three piezoelectric stacks and the holders for the PCB on top. 36
6.2 Another early stage sketch of the prototype. 37
6.3 Sketch showing different options that could be used to counteract the shear stress on the actuators. 38
6.4 The last sketch before making a CAD drawing. It was decided to use two separate modules, one that holds the image sensor board using the piezoelectric stacks, and one that holds the lens. 39
6.5 The base of the bottom plate where the actuators sit. Note the screw holes and the cut outs for the chords for each stack. 40
6.6 Image sensor board holder for M3065/85 camera. Note the long structures where the piezoelectric stacks would sit. This structure was shortened in another version of the prototype. 40
6.7 The lensholder with a cutout for the image sensor. . . . 41

6.8 Mounting plate for the whole structure. The screw holes on the side holds the large PCB. 41
6.9 The complete set-up for the M3065/85 camera. Note the structures surrounding the stacks that was not used. 42
6.10 The final prototype with the M3088 camera without the mounting plate. Note that the support structure for the piezoelectric stacks are shortened. 43
6.11 The final prototype parts printed out using a 3D printer. 44
6.12 The image sensor board holder with and without the board in. a) shows the board holder, and b) shows the board holder with the board in it. 44
6.13 The 3D printed parts attached to the piezoelectric stacks. The picture in a) represents the stacks placed in their holder with the board holder placed on top. The picture in b) represents the stacks placed in their holder. . 45
6.14 The 3D printed lensholder-structure. Note the protruding structures around the sensor-cutout that establish the correct distance between the lens and sensor. 45
6.15 The placement of the three piezoelectric stacks. 46
6.16 Schematic representation of the sensor board being tilted by the pressure of the piezoelectric stacks. 47
6.17 a) The piezoelectric stacks from the side when the two bottom stacks are fully extended. The black line is the sensor board. The second image shows the stacks seen from above. The dotted lines mark the limiting edges where the sensor board is supported by the stacks. b) Same as in a) but when the top stack is fully extended. 47
6.18 The piezoelectric stacks seen from the side, when the dotted stack is fully extended. The distance L is the distance between the two limiting edges of the stacks. The distance d is the displacement. The angle α is the amount of tilt. The grey piece in between the stacks marks approximately where the sensor sits on the sensor board. 48
6.19 The sensor (grey) will not move the entire distance of the displacement from the extended piezoelectric stack. 49

6.20 When the sensor board is tilted a strain will be put on to the piezoelectric to move. The movement is illustrated by the arrows and dotted piezoelectric stack. 49
6.21 A piezoelectric stack with an end hemisphere from Thorlabs [24]. 50

8.1 The plot of the corner focus test of the manual set-up of the M3085/M3065 camera. The standard deviation is also plotted. For example upper left corresponds to the upper left corner in the image. 57
8.2 The plot of the corner focus test of the first prototype with the M3085/M3065 camera. The standard deviation is also plotted. In a) a better focus value is achieved when the voltage is increased. In b) a better value is achieved when the voltage is low. The standard deviation is also plotted. 58
8.3 The plot of the corner focus test of the manual set-up of the M3088 camera. The standard deviation is also plotted. 59
8.4 The plot of the corner focus test of the manual set-up of the M3088 camera. The standard deviation is also plotted. In a) a better focus value is achieved when the voltage is increased. In b) a better value is achieved when the voltage is low. The standard deviation is also plotted. 60
8.5 Images of whiteboard with Siemens stars. a) displays the image when the piezoelectric stacks have a voltage of 0 V. b) displays the image when the piezoelectric stacks have a voltage of 150 V. 61
8.6 Zoomed in images of the center of the whiteboard. a) displays the image when the piezoelectric stacks have a voltage of 0 V. b) displays the image when the piezoelectric stacks have a voltage of 150 V. 62
8.7 Zoomed in images of the left corner of the whiteboard. a) displays the image when the piezoelectric stacks have a voltage of 0 V. b) displays the image when the piezoelectric stacks have a voltage of 150 V. 62

8.8 Zoomed in images of scribbles on the whiteboard. a) displays the image when the piezoelectric stacks have a voltage of 0 V. b) displays the image when the piezoelectric stacks have a voltage of 150 V. 63
8.9 Manual set-up of the M3085/65 camera. (a 0 μm (b Sensor moved 41μm away from the lens. 63
8.10 Manual set-up of the M3085/65 camera. a) Center of image 0 μm away from the starting point. b) 41 μm away from the starting point. 64
8.11 Manual set-up of the M3085/65 camera. a) Left upper corner of image 0 μm b) Left upper corner of image moved 41 μm away from the lens. c) Right upper corner of image 0 μm d) Right upper corner of image moved 41 μm away from the lens 64
8.12 Manual set-up of the M3085/65 camera. a) Left upper corner of image 0 μm b) Left upper corner of image moved 41 μm away from the starting point. c) Right upper corner of image 0 μm d) Right upper corner of image moved 41 μm away from the starting point. . . . 64
8.13 Manual set-up of the M3085/65 camera. (a 0 μm (b Sensor moved 41 μm away from the starting point. 65
8.14 Manual set-up of the M3085/65 camera. a) Center of image 0 μm away from the starting point. b) Center of image 40 μm away from the starting point. 65
8.15 Manual set-up of the M3085/65 camera. a) Left upper corner of image 0 μm b) Left upper corner of image moved 41 μm away from the starting point. c) Right upper corner of image 0 μm d) Right upper corner of image moved 41 μm away from the starting point. . . . 66
8.16 Manual set-up of the M3085/65 camera. a) Left lower corner of image 0 μm b) Left lower corner of image moved 41 μm away from the starting point. c) Right lower corner of image 0 μm d) Right lower corner of image moved 41 μm away from the starting point. . . . 66
8.17 Manual set-up of the M3088 camera. a) 0 μm b) 20 μm c) 40 μm. 67
8.18 Manual set-up of the M3088 camera. Super close up of center of a siemens star. a) 0 μm b) 20 μm c) 40 μm . . . 67

8.19 Manual set-up of the M3088 camera. Close up of chairs at a far distance. a) 0 μm b) 20 μm c) 40 μm 67
8.20 Images taken using Prototype 2. The image in a) is taken at 0 V and in b) at 150V. 68
8.21 Zoomed in mages taken using Prototype 2. The image in a) is taken at 0 V and in b) at 150V. 68
8.22 Zoomed in mages taken using Prototype 2. The image in a) is taken at 0 V and in b) at 150V. 69
8.23 Zoomed in mages taken using Prototype 2. The image in a) is taken at 0 V and in b) at 150V. 69
8.24 An image of a hallway taken with the M3088 Prototype 2. The voltage across the piezoelectric stacks were a) 0 V and b) 150V. 70
8.25 Close up of a the Siemens star close to the camera in Figure 8.24 Taken with m3088 Prototype 2. The voltage was a) 0 V b) 150V 70
8.26 Close up of a the Siemens further away from the camera in Figure 8.24 Taken with m3088 Prototype 2. The voltage was a) 0 V b) 150V 71
8.27 Close up of a the Siemens star furthest away from the camera in Figure 8.24 Taken with m3088 Prototype 2. The voltage was a) 0 V b) 150V 71
8.28 A person at a distance of 18m away from the camera. The image is taken by the M3088 prototype 2. Close up can be seen in 8.31. 72
8.29 A person at a distance of 6m away from the camera. The image is taken by the M3088 prototype 2. Close up can be seen in 8.32. 72
8.30 A person at a distance of 3m away from the camera. The image is taken by the M3088 prototype 2. Close up can be seen in 8.33. 73
8.31 Close up taken by the M3088 prototype 2 at a) 0 V and b) 150V. The full image of a) can be seen in Figure 8.28 . 73
8.32 Close up taken by the M3088 prototype 2 at a) 0 V and b) 150V. The full image of a) can be seen in Figure 8.29 . 74
8.33 Close up taken by the M3088 prototype 2 at a) 0 V and b) 150V. The full image of a) can be seen in Figure 8.30 . 74

8.34 Graph showing the hysteresis in the piezoelectric stacks captured in the focus values of the images taken from 0-150V with steps of 5V. 76
8.35 Graph depicting a worsening in the focus of the image when applying a voltage to the stacks. Note the yellow line (Left lower corner), having the biggest change of focus. 77
8.36 Images at a) 0 V on all the piezoelectric stacks, and b) 150V on all the stacks. Note the worsening of the quality in the latter image. 78
8.37 Zoomed in images of the center Siemens star at a) 0 V on all the piezoelectric stacks, and b) 150V on all the stacks. Note the worsening of the quality in the latter image. 79
8.38 Zoomed in images of the left lower corner Siemens star at a) 0 V on all the piezoelectric stacks, and b) 150V on all the stacks. Note the worsening of the quality in the latter image. 79
8.39 Graph depicting a bettering in the focus of the image when applying a voltage to the stacks. Note the blue line (Center), having the biggest change of focus. 80
8.40 Images at a) 0 V on all the piezoelectric stacks, and b) 150V on all the stacks. Note the obvious over all improvement of the quality in the latter image. 81
8.41 Images zoomed in at the center Siemens star at a) 0 V on all the piezoelectric stacks, and b) 150V on all the stacks. Note the obvious over all improvement of the quality in the latter image. 82
8.42 The Center focus values from the test in Figure 8.43. This specific test shows the focus value peak. 82
8.43 The focus-graphs for different regions when running the focus algorithm. Note the large difference for the different regions. The corresponding values can be found in Table 8.2. 84
8.44 The focus-graphs for different regions when running the focus algorithm. Note the large difference for the different regions. The corresponding values can be found in Table 8.3. 86

8.45 A screenshot of oscilloscope measurements of the current is shown, captured at the moment when the controller connected to a piezoelectric stack is turned on. The y-axis depicts the current and the x-axis the time. The figure depicts the stack charging up and acting as a capacitive interrupt after the charging process. Note that the current peak lasts for 85-90 ms. 89
8.46 A screenshot of oscilloscope measurements of the current is shown, captured at the moment when the controller connected to a piezoelectric stack is turned on. The y-axis depicts the current and the x-axis the time. The figure depicts the stack discharging and acting as a capacitive short circuit after the discharging process. Note that the negative current peak lasts for 85-90 ms . 89
8.47 A screenshot of oscilloscope measurements of the current is shown, captured when the controller is turned off and no current, except for a slight offset of 400 μm, is running through the circuit. The y-axis depicts the current and the x-axis the time. 90
8.48 A screenshot of oscilloscope measurements of the current is shown, captured when the controller has been turned on at 150V for a while. Note the current of 950 μm running through the circuit. The y-axis depicts the current and the x-axis the time. 90

List of Tables

4.1 Piezoelectric stack specification [26]. 20
4.2 M3065 Camera specifications [4] 22
4.3 M3088 Camera specifications [5]. 23

8.1 Focus values and ratios when running the focus algorithm on the prototype from the test in Figure 8.39. . . . 83
8.2 Focus values and ratios when running the focus algorithm on the prototype from the test in Figure 8.43. . . . 85
8.3 Focus values and ratios when running the focus algorithm on the prototype from the test in Figure 8.44. . . . 86
8.4 Focus values and ratios when deliberately tilting the sensor. Note the bottom and and top ratios. 87
8.5 Oscilloscope measurements of current figures 8.47 and 8.48. 90

List of Abbreviations

PZT	Lead Zirconate Titanate
RAM	**R**andom **A**ccess **M**emory
RGB	**R**ed **G**reen **B**lue
MTF	**M**odular **T**ransfer **F**unction
SFR	**S**pacial **F**requency **R**esponse
RoHS	**R**estrictions (of) **H**azardous **S**ubstances
POE	**P**ower **O**ver **E**thernet
WDR	**W**ide **D**ynamic **R**ange
ROI	**R**egion **O**f **I**nterest
PCB	**P**rited **C**ircuit **B**oard
KNN	Potassium Sodium Niobate

Chapter 1

Introduction

1.1 Background

Axis Communications AB is a Lund based company, founded in 1984. They have been the industry leader in network-based video surveillance since the launch of the world's first network camera in 1996. Now, Axis offers a large variety of network cameras and audio, as well as access control.

One of the major challenges in the production of imaging devices is ensuring that the imaging sensor and lens are properly aligned, and Axis Communications' cameras are no exception to that problem. Misalignment of these components results in blurry images, which can affect the quality of the final product. The alignment is done during the production process and cannot be adjusted afterwards. If the image quality is severely affected by misalignment, due to external force or extreme temperature on the site, the product must be returned, ultimately resulting in additional costs for Axis.

To address this issue, Axis have been exploring ways to prevent the misalignment using piezoelectric elements. Piezoelectric elements are materials that can change shape when exposed to a voltage. By using these elements, the camera could self-regulate in order to make precise adjustments to the position of the sensor and lens automatically. This can greatly reduce the likelihood of misalignment and improve the overall image quality of the product.

Overall, the use of piezoelectric elements in the alignment of imaging sensors and lenses has the potential to improve the quality of imaging devices and reduce costs for Axis. The company is constantly researching and experimenting with new ways to implement this technology in the production process to ensure the best results for the customers. This master's thesis hopes to be the starting point in future implementation of piezoelectric components for sensor alignment. Thus, the company is committed to delivering high-quality products and is always looking for ways to improve and innovate to stay ahead of the competition [1].

1.2 Goals

In order to investigate the possibility of implementing a piezoelectric element into the company cameras to stabilize the focus of the lens, the following milestones needs to be achieved:

1. **Do a case study**

   Research and purchase the appropriate piezoelectric element needed to fulfill the specific camera standards. In order to fulfill this goal, the camera standards must be investigated; What temperature does it work in? How much space is there to fill? And more specific: How much displacement does the element need to achieve? How many dimensions and how many microns?

2. **Build a prototype and test it.**

   Does the set-up meet the standards? Can it be controlled (manually)?

3. **Implement digital control.**

   Make an algorithm that regulates the alignment of the sensor to the lens automatically.

To summarize, the goal is to successfully document what type of piezoelectric element is most suitable for the application, how the implementation should be done, what algorithms the element should use as well as which of Axis's cameras would benefit most from the addition of a piezoelectric element.

Chapter 2

Theory

2.1 The Piezoelectric Effect

The piezoelectric effect was first documented in 1880 by Jacques and Pierre Curie, when they discovered that a quartz crystal could generate electric potential when exposed to pressure. They named the discovery "piezo effect", as the word "piezo" is derived from the Greek word for pressure. More specific, is this phenomenon called the *direct* piezoelectric effect, while the opposite, when electric potential is converted into mechanical energy is called the *inverse* piezoelectric effect [7].

This phenomenon can be found in some natural occurring materials, but manufactured piezoelectric materials have more advanced material properties and are therefore able to achieve more gain. One common type of manufactured piezo electric material is the polycrystalline ferroelectric ceramic material, Lead Zirconate Titanate (PZT). To be able to achieve piezoelectric properties the PZT needs to be polarized. This allows the positive and negative ions to separate and display the electric dipole behavior of the piezoelectric effect [7].

2.1.1 Crystal Structure

Piezoelectric materials uses mechanical energy to convert to electrical energy thus an applied strain or stress induce a change in polarization due to the piezoelectric effect. In randomly oriented materials, there is no net polarization; The polarization is fixed by the crystal structure

and cannot be reoriented without the breaking of bonds. The most common piezoelectric ceramics (including PZT) has the perovskite crystal structure [27]. Figure 2.1 shows the perovskite crystal structure, with and without an applied external electric field.

Lead Zirconate Titanate

The most common material used when aspiring to use piezoelectric properties is PZT, a solid amongst $PbTiO_3$ and $PbZrO_3$, see Figure 2.1. PZT has a high Curie temperature (the temperature at which the piezoelectric properties are lost), making it a good candidate for uses at high temperatures. It is also highly polarizable; It can sustain a strong electric field without breaking down. Furthermore, PZT has good mechanical and chemical stability, making it resistant to fatigue and degradation over time [13].

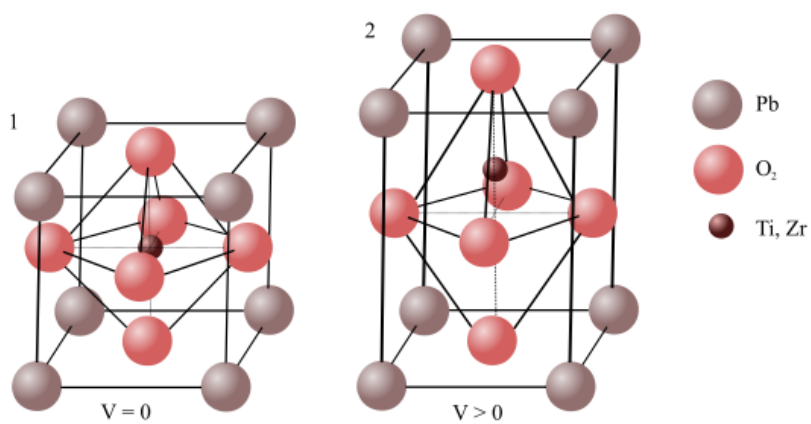

FIGURE 2.1: Perovskite crystal structure of PZT. Structure one is the lattice at 0V, and structure two is the lattice with an applied voltage.

PZT can be easily fabricated into various shapes and sizes, which

makes it suitable for a wide range of applications thus its unique combination of properties makes it an ideal material for piezoelectric applications [13].

2.1.2 The Piezoelectric Actuator

The piezoelectric actuator is an actuation device, that converts electrical energy into motion [17]. It uses the inverse piezoelectric effect, meaning it uses an electrical charge to preform a mechanical movement. The demand for nanoscale accuracy in positioning technology is critical now more than ever. Properties such as high speed, long working distance, stable performance and more compact structures are greatly appreciated and can be achieved with piezoelectric actuators. Today, these are most often made from soft PZT ceramics. Their intrinsic properties of high strain-electric field hysteresis (ca 15%) and a piezoelectric coefficient of 500-700pC/N leads to high drive voltages [11].

One type of actuator is the multilayered piezoelectric actuators or piezoelectric stacks, where layers of piezoelectric materials are stacked alternating with electrodes. This type of actuator requires a relative low drive voltage and a small volume to achieve a large output force [11].

2.2 The Functionalities of a Camera

Two essential components the cameras used in this project are a lens that focuses the light, as well as a component to capture it and turn it into a digital signal called an imaging sensor. There are many important factors that affect the sharpness of an image, for example the size of the pixels in the sensor, the size and thickness of the lens, the distance between the two etc. The lens focuses the light into a focal point and this is where the sensor should be. The distance from the lens to this point is called the focal length [20].

2.2.1 The Lens

F-number

The entrance of the lens is called the clear aperture and the area of the clear aperture is directly proportional to the amount of light collected. At the sensor, the illumination, measured in power per unit area, is inversely proportional to how large the enlightened area is, which is proportional to the square of the focal length f. The area of the clear aperture is proportional to the square of the diameter of the pupil D. The $f - number$ is the ratio of the focal length to the clear aperture and can also be called the relative aperture [20].

$$f - number = \frac{f}{D} \tag{2.1}$$

The relative illumination produced in a image is inversely proportional to the square of the f-number. Therefore a low f-number means a higher amount of light. For example a lens with a 8 inch focal length and 1 inch clear aperture will have an f-number of $8/1 = 8$ often written as f/8 or f:8 [20].

Barrel Distortion

Wide-angle cameras have the benefit of capturing a wide range of field. However, a downside to the wide angle is that it is prone to a type of distortion called the barrel distortion, where the image seems to be mapped around a barrel, see Figure 2.2. This is due to the lens not being completely ideal meaning the magnification factor is not ideal. The magnification factor increases towards the optical center in particular for lenses with short focal length such as wide-angle lenses [12].

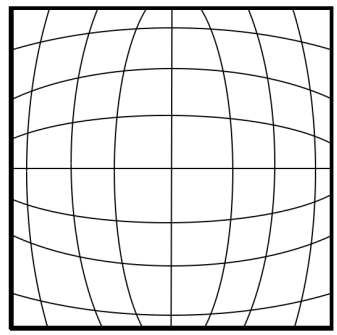

FIGURE 2.2: This is how an image gets distorted by barrel distortion.

2.2.2 The Image Sensor

An image sensor converts incident light, in the form as photons, into electrical charge, then measures it and converts it to a readable signal. A CMOS sensor is built up of photosites that consists of photodiodes with an adjacent charge-to-voltage converter. Depending on how advanced the device is, other preprocessing circuits, such as an amplifier, can also be present. The photosites are placed as an 2D matrix and connected as a 2D array where built-up voltage is collected and transferred to an output node. The output is saved in random access memory (RAM) which uses an row-column based mechanism [18].

A sensor that uses progressive scan uses a technique where every vertical line in an image is fully scanned every time. Compared to the technique interlace technology, where the image is divided into fields and only half the fields are scanned at a time, progressive scans give a more clear image and reduces motion blurring [2].

As the sensor in it self is "colorblind", a filter is therefore placed in front of it which allows each pixel to be assigned a specific color tone. The human eye is most sensitive to green light compared to blue and red, it is therefore common that the filters favor the color green as this makes it possible to see more details compared if the colors were favored equally. One of the most common filters that uses the RGB

"Red, Green and Blue" color registration method is the Bayer array. More specifically, it uses alternating rows of red and green, and blue and green as seen in Figure 2.3. This means that four pixels is needed to complete a full group [3].

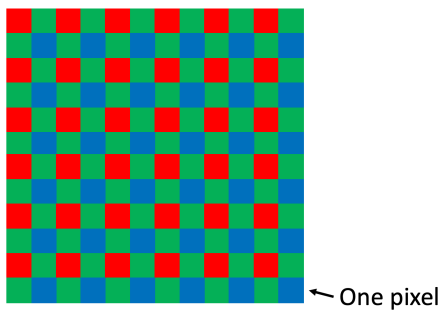

FIGURE 2.3: An example of a Bayer filter

2.3 Focus Measurements

2.3.1 The Laplacian Operator and its Variance

The Laplacian operator is a second order derivative filter and is used when one would want to discover sharp edges in an image. It is especially effective in digital image processing thus it highlight areas of fast changes in intensity; When an image is in focus, the edges are sharp, thus the intensity changes rapidly and the Laplacian operator gives a high response. There are positive and negative kernels to use, each of which are effective for detection of edges. In the positive Laplacian operator the corner elements of the mask are set to zero, and the center element is set to a negative value. The remaining elements of the mask can be set to either zero or a positive number. In the negative Laplacian operator however, the corner elements are set to zero, the center element is set to a positive value, and the remaining elements of the mask are set to -1 [6].

When computing the variance of the image after applying a Laplacian mask gives an indication of how much edge detail there is. A high

variance means that there are a lot of responses to sharp edges. If an image has few of those, the image is considered blurry [6].

2.3.2 The Modulation Transfer Function

When testing the performance of optical systems a common target to use is alternating bright and dark stripes of the same thickness, see Figure 2.4 a). One way to use these targets is to have sets of stripes with different thickness. The size of the thinnest lines the system can discern is regarded to be the limits of the resolution and expresses as the number of lines per millimeter, where one line consists of a pair of a dark and light bar [20].

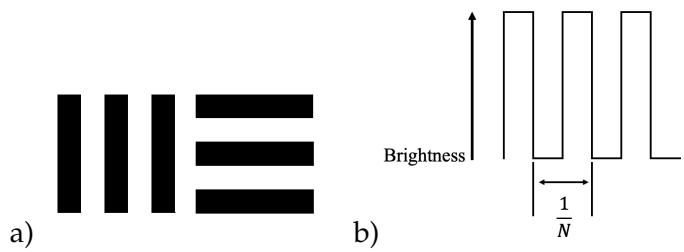

FIGURE 2.4: a) An example of a common pattern used as a target for testing performance of optical systems. b) The brightness of the target. 1/N indicates the number of stripes per millimeter.

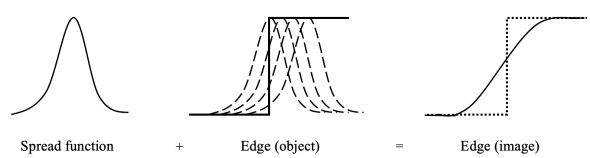

FIGURE 2.5: The spread function creates a blurred effect across edges.

The point spread function describes how the light is distributed in an image of a point and shows how the illumination is highest in the center of the point and then fades. An image can be described as a summation number of multiple points spread function. When the target in Figure 2.4 a) is imaged, the edges are blurred by the line spread function, see Figure 2.5. As the pattern gets finer the patterns becomes more blurred. When the optical system can no longer detect the illumination contrast the pattern is not able to be resolved. The contrast can be expressed as "modulation", and calculated by:

$$Modulation = \frac{max. - min.}{max. + min.} \tag{2.2}$$

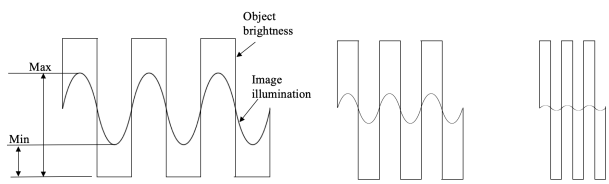

FIGURE 2.6: When the test pattern (square wave) becomes smaller, the contrast in the image (sine wave) becomes smaller.

Where max. is the highest illumination level and min. is the lowest, see Figure 2.6. The modulation is often plotted as a function of the line frequency, where a higher frequency means thinner lines and therefore also more lines per millimeter. The smallest modulation the optical systems sensor can detect can also be plotted as a function of frequency, and the interception between these two lines limits the resolution. However, the performance of a system can differ from another even if the limiting resolution is the same. For example one system can have much higher modulation at lower frequencies than another. Determining which system has the best performance is not trivial, one system may give a higher modulation at low contrast than another, but may also have a higher limiting frequency, see Figure 2.7

b). In these cases the importance of resolution in relation to contrast will determine the most suitable system [20].

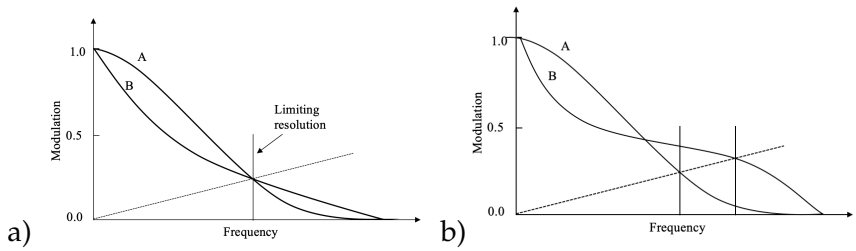

FIGURE 2.7: a) The system A and B has the same limiting resolution but A will produce a better image at low frequencies. b) System A will produce a better image at low frequencies but system B has a higher limiting resolution. The most suitable system must be based on the application.

The example with the test target describes the brightness as a squared wave function and the image illumination as the distorted square wave with rounded off corners. If the brightness distribution of an object is instead described with an sine wave the distribution in the images will also be a sine wave. This has made made the modulation transfer function (MTF) a common method to determine the performance of a lens system.

$$MTF(v) = \frac{M_i}{M_o} \tag{2.3}$$

Where M_i is the modulation in the image and M_o is the modulation of the object and v is the frequency [20].

Spatial Frequency Response

One common way to measure performance of digital imaging is by using the MTF concept but adapted and applied to become the spatial frequency response (SFR) [30].

2.4 Electrical Properties

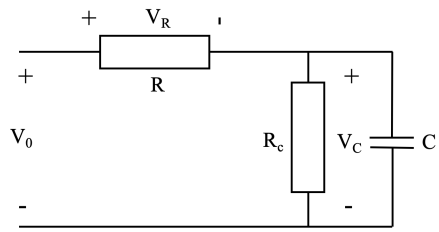

FIGURE 2.8: Wiring diagram of the resistors and a capacitance.

As an electrical component the piezoelectric stack can be compared to a capacitor [9]. When a voltage is applied there is a voltage difference between the two sides of the stack and no current pass through except when the voltage is changed and the stack is charged or uncharged. In Figure an example of a circuit with a piezoelectric element and two resistors R_C and R can bee seen. If $R_C >> R$ the time it takes to charge a capacitance in the circuit can be described as:

$$v_C(t) = V_0(1 - e^{-t/RC}) \tag{2.4}$$

Where $v_C(t)$ is the voltage over the capacitor for the time t, V_0 is the voltage over the circuit, R is the resistance and C is the capacitance. This equation assumes that the capacitance is uncharged $v_C(t) = 0$ at the starting time t=0.

When the voltage source is disconnected the capacitor will discharge through the resistor R_c. The time it take for the resistor to discharge can be described by:

$$v_C(t) = V_0 e^{-t/RC} \tag{2.5}$$

When t becomes infinitely large the piezoelectric stack is fully charged and no current can pass though the device and it can be described as an open circuit. The same amount of voltage will drop across both

the resistor and the stack as they are parallel to each other. The two resistors will be in series.

The voltage drop V_C can be described by:

$$V_C = R_c \cdot I = V_0 \frac{R_c}{R + R_c} \tag{2.6}$$

The amount of energy a component consumes can be described by the power consumption and time [8].

$$p = V \cdot I \cdot t \tag{2.7}$$

Chapter 3

Market Analysis

3.1 Requirements

To choose a suitable piezoelectric device for the purpose of this project, a study had to be carried out. The following aspects were taken into consideration:

- Price within the given budget.
- Reasonable size to be feasible in a camera prototype set-up.
- Shipping time of no more than 2 weeks.
- Displacement of the element should be at least ± 20 microns.
- Easy usability and implementation.
- Match the specifications of the camera regarding temperature (-20$^{\circ}C$ - +60$^{\circ}C$).

3.2 Types of Piezoelectric Devices

It seemed that only one manufacturer could provide a short enough shipping time, so further studies were made on the elements on their website.

After further research, more consideration was put into the technical specifications of the elements and it was concluded that capacitance

was not a big issue thus the wanted implementation does not call for fast and voltage-robust elements. The biggest issue became the balancing of size and possible displacement of the element as well as the ease of implementation of the element. After some research the market was narrowed down to three types of alternatives: piezo motors, amplified piezoelectric actuators and piezoelectric stacks. Piezo motors are devices that in some way or another uses the piezoelectric effect in order to emphasize the movement of a surrounding structure, and thus provides a large displacement without compromising size and are self locking at rest. However the implementation in a simpler prototype and their high price tag quickly became a moment of concern [7]. Amplified piezoelectric actuators are flexure housing with a piezoelectric stack mounted inside it, see Figure 3.1. They have a much larger displacement than needed, and they would have been bulky to use as in this set-up as it was of desire to use three elements in order to be able to tilt. They are also expensive [25].

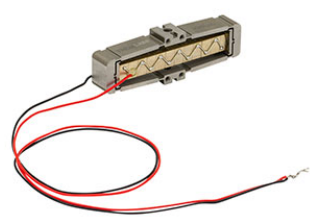

FIGURE 3.1: Amplified piezoelectric actuators from Thorlabs. The size is 14.0 x 7.0 x 44.0 mm [25].

Simple piezoelectric stacks (see Figure 4.1) seemed to be the cheapest and simplest to implement, and by observing the different alternatives, the length of the element implied to be linear to the displacement. As a displacement of at least 40 μm in total was needed, a stack of at least 36 mm was of interest.

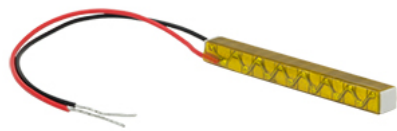

FIGURE 3.2: The piezoelectric stack used from Thorlabs [26].

.

Almost all options, whether they be a simple stacks or a motor, are made from a crystal containing lead. As of 2023 the "Restriction of Hazardous Substances in Electrical and Electronic Equipment" (RoHS) allows for only 0.1 % lead in a homogeneous material, but an exception is made for piezoelectric devices; A piezoelectric stack is allowed to contain more than 0.1% lead [15]. With this in mind, the chosen piezoelectric crystal is in the form of a piezoelectric stack that was bought from Thorlabs [26] and its specifications can be found in Table 4.1.

In the market analysis some lead free alternatives was found, but none that had a displacement of 40 μm. The ones that was found only had a displacement of a couple of microns and were more expensive than the ones that was bought.

Chapter 4

Materials

4.1 Discrete Piezoelectric Stacks

Discrete piezoelectric stacks from Thorlabs are made by placing multiple piezoelectric chip on top of each other and bonding them together with glass-bead epoxy. This in order to maintain the fast response time but also achieve a larger displacement. The stacks are then also able to achieve sub-millisecond response times all at relatively low drive voltage range (0V-150V). Each individual chip in the stack is protected by a ceramic barrier layer, which gives a good resistance to humidity and heat [26].

The chips have alternating internal electrodes with opposite polarities, where the electrode layer is shorter than the piezo layers full width, as seen in Figure 4.1. The electrodes are flushed to one side and do not reach the opposite side. All the electrodes with the same polarities are connected to the same side and the electrodes with the opposite polarities are connected to the opposite side. This makes each electrode's far side surrounded by PZT material and isolates it from the from the opposite polarity supply electrode. A result of this is that a region of stress is created at the edge of the electrode due to both the change in thickness on the alternating sides and the tensile stress from the PZT material responds to an external voltage when the PZT on the edges do not. The height of a chips is limited by this stress so that internal stress is not high enough to affect the lifetime or performance of the chip.

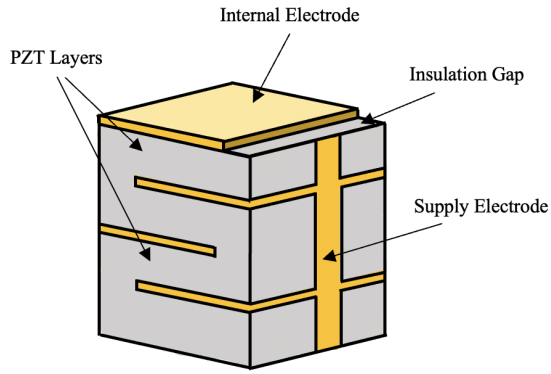

FIGURE 4.1: Schematic of the stacks used from Thorlabs.

4.1.1 Hysteresis and Individual Properties

The following specifications applies to the chosen piezoelectric stacks, see Table 4.1 [26].

TABLE 4.1: Piezoelectric stack specification [26].

Parameter	Value
Drive voltage range	0-150 V
Displacement (Free Stroke) at 150 V	41.0 μm $\pm$ 15 %
Hysteresis	<15%
Recommended load	400N
Blocking Force at 150 V	1000N
Capacitance	3500 nF $\pm$ 15%
Operating Temperature	-25 to 130 °C
Curie Temperature	230 °C
Outer Dimensions	5.2 mm x 7.1 mm x 36.0 mm
Piezo Stack Dimensional Tolerance	$\pm$ 0.1 mm

There are multiple factors where each piezoelectric stack may have individual properties. The size of the stack can vary with $\pm$ 0.1 mm and the displacement have a risk of differing with $\pm$ 15 % of 41 μm. As this is a larger difference than the maximum displacement this may create problems such as unwanted tilt of the image sensor board both with and without applied voltage.

Another problem with direct piezoelectric stacks is hysteresis, see Figure 4.2. The hysteresis means the actuators will have one displacement size when the voltage is increased and another when the voltage is decreased. This makes it impossible to know how large the exact displacement is, only knowing the applied voltage. Another problem is the maximum displacement length varies with $\pm$ 15% which further aggravates the difficulty of knowing the displacement.

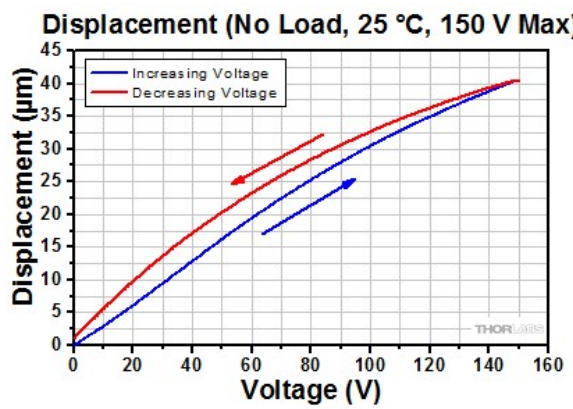

FIGURE 4.2: Figure showing the displacement vs the voltage. Note the 15% hysteresis [26].

One way to counteract the uncertainty in displacement is to use piezoelectric stacks with a strain gauge sensor and an inner regulation loop that makes sure the actuators have the wanted displacement. There would still be one outer loop that decides the wanted displacement based on the feedback from the image. The drawback of using this

set-up is that it is more complicated, more expensive and more equipment is required. The outer loop would still decide the size of the displacement based on the information from the image. Therefore, the knowledge of the exact displacement size is not necessary. It might be beneficial to be able to compare and control the actuators more precisely in relation to each other. However, as a first prototype the knowledge from the image should be enough.

4.2 The Cameras

4.2.1 M3065 & M3085

The camera used in the first part of the project was a combination of a Axis M3085-V and M3065 Dome Camera . The image sensor was from a M3065 camera, while the lens-package and main board was from a M3085 camera. Its specifications can be found in table 4.2 [4]. This camera does not have the function to change the focus remotely.

TABLE 4.2: M3065 Camera specifications [4]

Image sensor	1/2.9" progressive scan RGB CMOS
Lens	3.1 mm, F2.0 Fixed iris, IR corrected
Operating conditions	0°C- 45°C
Resolution	1920x1080 (1080p) to 320x240
Power	Power over Ethernet (PoE) Type 1 Class 1 Typical 2.2 W, max 2.5 W

4.2.2 M3088

The Axis M3088 dome camera, being an M-line camera, is one of Axis most cost-effective cameras. It has 8MP image quality and wide dynamic range (WDR). In Table 4.3, specific specifications are listed [5]. The dome covering the lens, as seen in Figure 4.3, gives the camera its name.

FIGURE 4.3: The Axis M3088 Dome camera [5].

TABLE 4.3: M3088 Camera specifications [5].

Image sensor	1/2.8″ progressive scan RGB CMOS
Lens	2.9 mm, F2.0 Fixed iris, IR corrected
Operating conditions	0°C- 40°C
Resolution	3840x2160 (8 MP) to 320x240
Power	Power over Ethernet (PoE) Type 1 Class 2 Typical 3.6 W, max 4.2 W

4.2.3 Other equipment

Other Equipment purchased was three Piezo Controllers from Thorlabs, as seen in Figure 4.4, one for each piezoelectric stack. This, along with a common power supply "Power Supply for Three K-Cubes" as seen in Figure 4.5. The cubes had a maximum current supply of 7.5 mA.

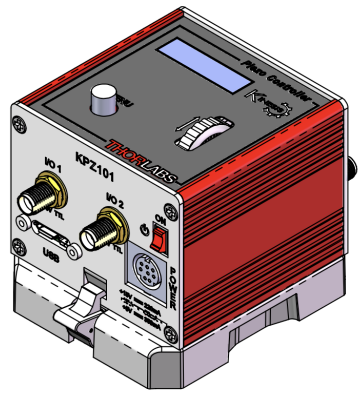

FIGURE 4.4: The Thorlabs KPZ101 - K-Cube Piezo Controller [23]. Note that three of these was used.

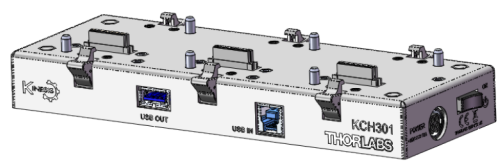

FIGURE 4.5: The Thorlabs KCH301 Power Supply for Three K-Cubes [22].

The remaining equipment that was used include three sets of 1 MΩ 1 kΩ and three SMA cables to connect the piezoelectric stacks with the controllers which is further discussed in Chapter 5, "Methodology".

Chapter 5

Methodology

5.1 Connecting the Piezoelectric Stacks

Two resistors were soldered to each piezoelectric actuator, see Figure 5.1. One 1 MΩ resistor parallel to the piezoelectric stack to make it possible to the stack to discharge; This was recommended by the supplier to have a resistor connected this way to protect the piezoelectric stack. The other resistor was a 1 kΩ and was connected in series with the stack, see Figure 5.2. This resistor acted as a precaution in case of a short circuit, as the voltage was quite high.

By equation 2.6 the voltage drop across the piezoelectric stack is:

$$V_C = V_0 \frac{1M\Omega}{1M\Omega + 1k\Omega} = 0.999V_0 \tag{5.1}$$

To be able to connect the resistors double ended SMA cables were cut and soldered to the cables of the stacks. It was important to connect the piezoelectric stack correct in relation to ground as reverse bias could destroy the stack. The other end of each SMA cable was connected to a piezoelectric controller from Thorlabs that was able to provide a voltage between 0 to 150 V to each piezoelectric stack. The three controllers were connected to a common power supply. The controllers was able to connect to a computer through a USB and be controlled by Thorlabs Kinesis user interface.

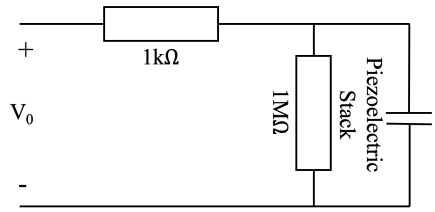

FIGURE 5.1: Wiring diagram of the resistors and piezoelectric stack.

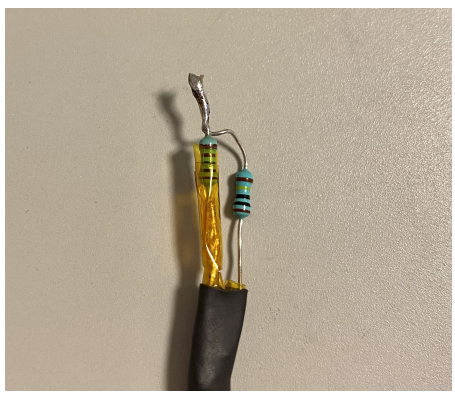

FIGURE 5.2: The two resistors attached on to an SMA cable before soldered onto a piezoelectric stack.

The current going through the resistors when the piezoelectric stack is charged will be:

$$I = \frac{V_0}{1k\Omega + 1M\Omega} \tag{5.2}$$

Where V_0 is the total voltage across the circuit. When the voltage is 150 V this will result in a current of 150 μA.

5.2 Siemens Stars

Prominent in almost all pictures taken are the Siemens stars, as shown in Figure 5.3. They consist of wide black strokes that becomes narrower towards the center where is the only place they actually meet [19].

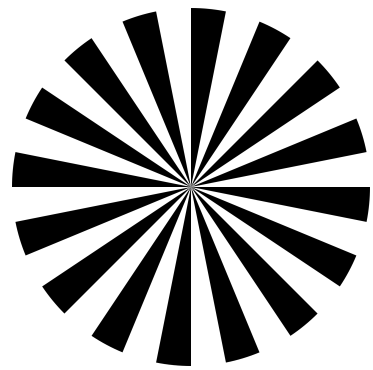

FIGURE 5.3: Siemens star that was placed in some of the images [29].

Depending on the resolution of the device, the "dot" in the center either becomes smaller for a better resolution and vice versa [19]. Moreover, this becomes vital when measuring the focus of an image both manually by looking at it, as used in Figure 5.4, but it also makes for a great target when running an focus algorithm.

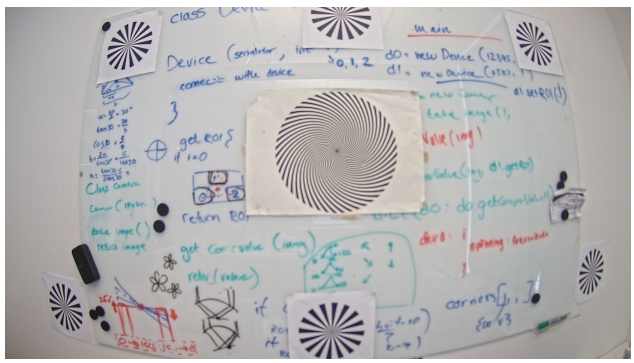

FIGURE 5.4: The usage of Siemens stars in a manual tests to make it easier for the naked eye to distinguish differences in focus. Note the blob in the middle of the Siemens stars indicating bad focus.

By constricting the regions of interests (ROI) to the Siemens stars in the field, as seen in Figure 5.5, a more accurate representation of the focus in all the ROI's is achieved, rather than having all the ROI's consist of different objects that could tolerate changes in focus differently and thus give a misrepresentation.

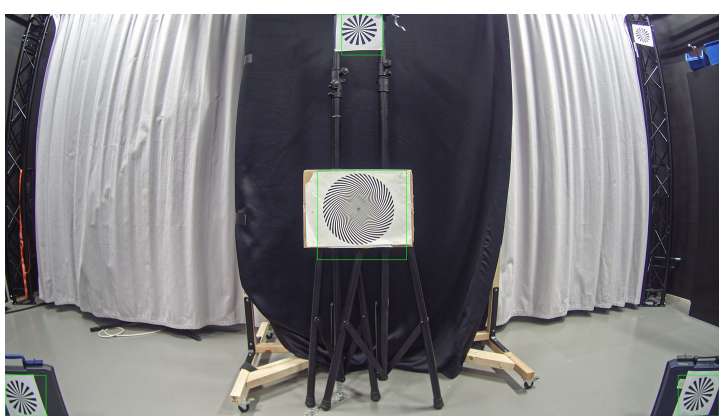

FIGURE 5.5: The defined ROI's are outlined in green and are used for the testing of the focus algorithm.

5.3 Characterization of the Prototype using HIT-Corner Focus Test and a Manual Stage

In order to characterize the prototypes, a few tests were made using them, but also using a controlled set-up as seen in Figure 5.6. This, not only to have a stable reference point when evaluating the prototypes, but also when using the manual stage, one will get a larger displacement of the length between the lens and image sensor and consequently a better overview of how sensitive the camera set-up used is for misalignment of the sensor. This enables for a better understanding of how the tests going forward are conducted; Where do one have to place the "initial" focus in order to do this?

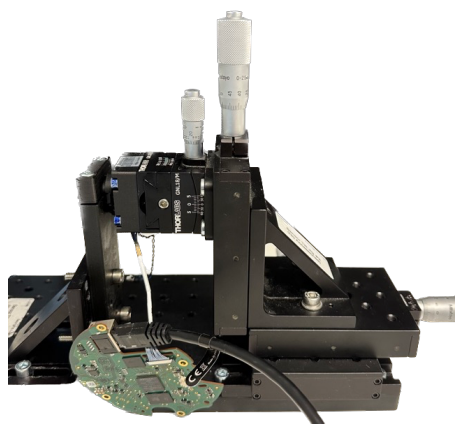

FIGURE 5.6: Thorlabs manual stage with a camera attached.

The reference set-up is made up from manual stages that makes it possible for us to, with $\sim 10\mu m$ precision, adjust the length between the image and the lens. The lens and image sensor printed circuit board (PCB) are fastened to separate 3D-printed holders that are screwed on to the stage from Thorlabs as seen in Figures 5.7 a) and b). Therefore the length between the sensor and the lens can be changed only by rotating the knob on the back of the stage and mimic the piezoelectric stacks in a more controlled fashion.

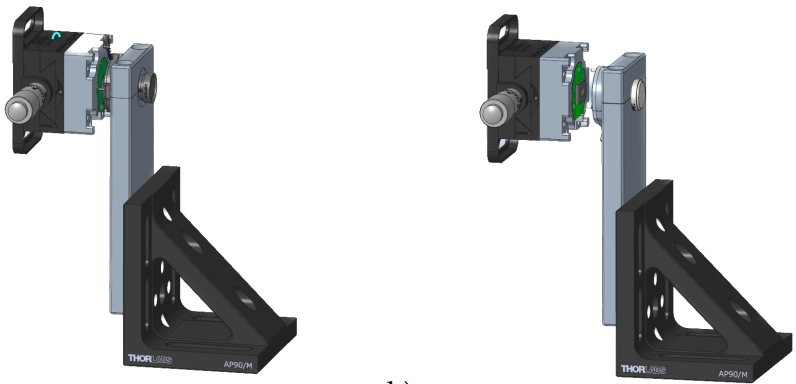

a) b)

FIGURE 5.7: CAD illustration of the parts that fit into the manual stage from Thorlabs. Figure a) is for the M3085/65 camera, and b) is for the M3088 camera.

By doing the HIT corner focus test on both cameras using the manual stages as well as the prototypes, quantitative data was collected that gives information of how good the prototypes were at changing the focus. The HIT tests were done in an image lab at Axis headquarter in Lund. The lab is set-up as a photography studio with controllable studio-lighting. The HIT test are done using an AXIS-made software. The target used in the test are seen in Figure 5.8.

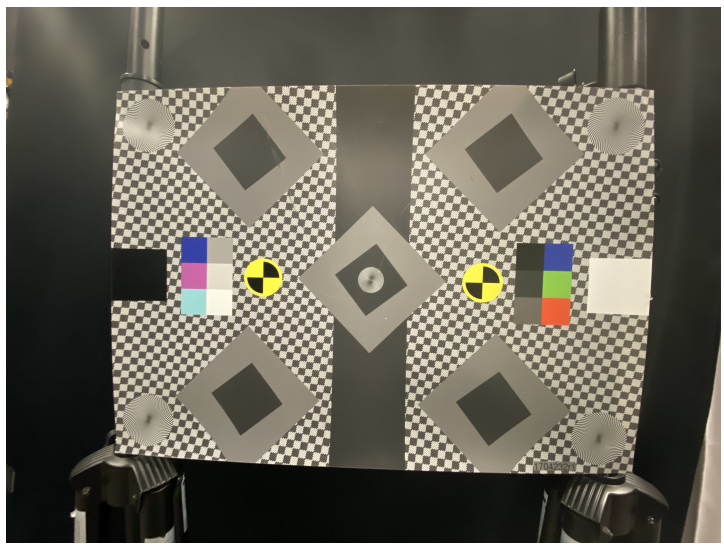

FIGURE 5.8: The target used in the HIT tests.

The prototype and the manual stage were placed around 35-40 cm from the target as seen in Figures 5.9 and 5.10. The targets were placed in front of a homogeneous, dark background. The test measures the SFR at 50 % amplitude in five different places, the center and each corner. A correctly aligned system should show equally sharp corners and a slightly sharper center.

Each test was done three times per set-up, starting over each time to avoid hysteresis. Furthermore for some tests, hysteresis was also measured by going backwards. The mean of the three tests were plotted for each set-up. Unfortunately one test for the manual set-up of the camera M3088 was lost, therefore only the mean of two test are used in that result. The results of the measurements are shown and discussed in Chapter 5.

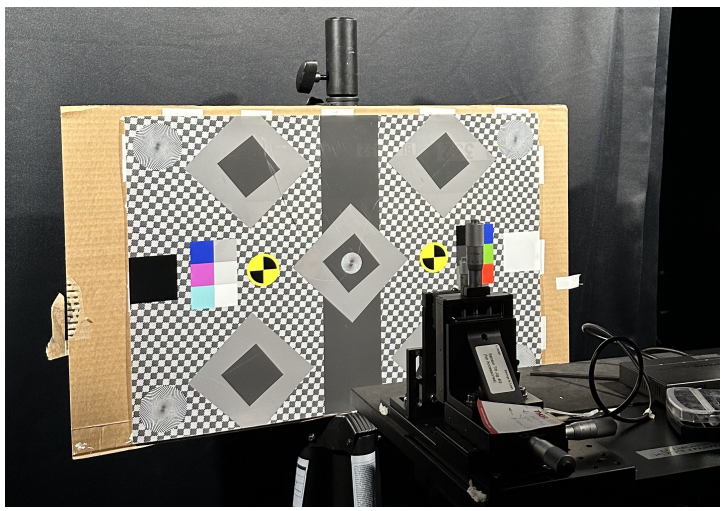

FIGURE 5.9: The HIT test set-up using the manual stage.

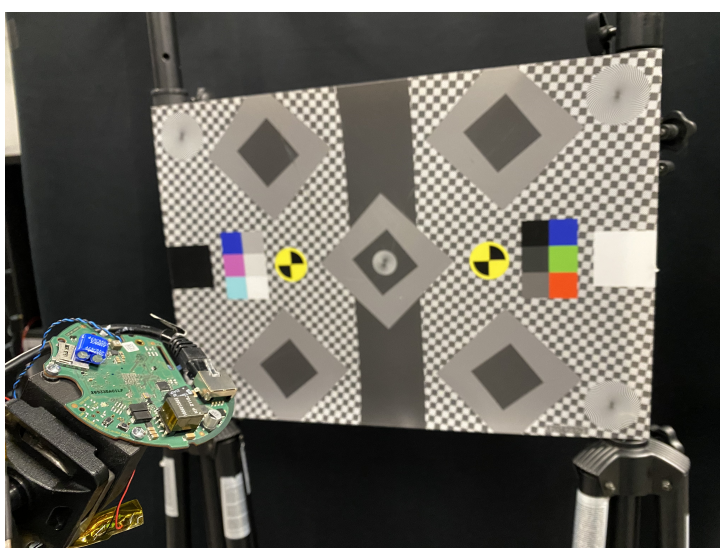

FIGURE 5.10: The HIT test set-up using the prototype.

5.4 Real Life Environments

5.4.1 Through a Window

The manual set-up for the M3088 used the same set-up as before, see Figure 5.7. The environment was the office and half the scene of the camera was faced towards a window and the other towards a wall covered with Siemens stars. The goal with this set-up was to compare the shift in focus in close distances and distances far away. The first image was taken with quite bad focus and then the sensor board was moved towards the lens in steps of 10 μm as the image quality increased. The images can be seen in Figure 8.17 - Figure 8.19 in Chapter 8.

Approximately the same view was used to take images with the M3088 prototype 2, unfortunately the same window was not available to use. However, the two views were similar as the window was in the same office. Another difference was that is was raining on the day of this experiment. The camera was placed in a position where the focus was not perfect but still good, but would be sensitive to small amount of movement of the sensor board towards the lens. Images were taken at 0V and 150V. The images can be seen 8.20 - Figure 8.23 in Chapter 8.

5.4.2 Along a Hallway

Images with the M3088 prototype 2 were taken in a hallway at the headquarter of Axis. The prototype was placed at the beginning of a hallway. The goal with the test was to investigate the focus at different distances. Both Siemens stars and a person were used as targets. The images can be seen 8.24 - Figure 8.32 in Chapter 8.

5.5 The Algorithm

To test the algorithm, images of four different Siemens stars were taken in the image lab. The position of each Siemens star corresponded to the region of interest used in the algorithm. The set-up used was the M3088 prototype 2 with a lens with a lower f-number of 1.2. It was important to keep the light controlled as well to make sure the three

ROI of the corners were alike. The comparison between the corner focus values would otherwise not be viable. The focus value of the top center corner, center, lower right corner and lower left corner was calculated. The center ratio to each of the corners and the means of all corners were also calculated as a indication of the tilt in the image. If the image sensor was perfectly aligned in relation to the lens, and the set-up was ideal would the ratio be 1. To read more about how the algorithm works see Chapter 7.

Tilting of the sensor was also tested by putting 150V across the two lower piezoelectric stacks and 0V across the top stack and vice versa.

5.6 Electrical Measurements

To measure the amount of current each piezoelectric stack consumes when charging (going from 0 V to 150 V), charged (stable at 150 V) and discharging (going from 150 V to 0 V) a current probe connected to an oscilloscope was used. The probe was put over one of the cords from the stack as the stack was connected to a controller. The results can be seen in Figure 8.45 - Figure 8.48.

Chapter 6

Prototype set-up

6.1 The Prototype

6.1.1 Idea and Requirements

It was decided to use 3D-printing to construct a prototype. The material in the printer was a type of plastic combine with micro carbon fiber filled nylon which made it resistant to heat and deformation up to a temperature of 145 °C [14].

When building the prototype there was a couple of things that had to be kept in mind. Most important was to consider that the piezoelectric stacks only can carry load in the y-direction and should not be exposed to any shear stress.

The idea was that the piezoelectric stacks would be attached to a bottom plate and a structure holding the PCB with the image sensor. In this set-up the stacks would be in a horizontal position and the weight from the attached PCB would put a shear stress on the stacks. To avoid this the first thought was that the stacks would be put into surrounding support structure. Another early idea of precaution to avoid shear stress on the stacks caused by the PCB was to introduce springs and placing them on the perimeter of the PCB. Both these ideas was later discarded as the total weight of the sensor PCB was thought to be light enough to not put a stress on the piezoelectric stacks.

6.1.2 Early stages

The first sketch made is shown in figure 8.5. In this simple sketch, a socket joint would be used between the piezoelectric stacks and the holders of the PCB. The socket joint would shield the stacks from shear stress from a tilted image sensor-board. This idea lacked a couple of things: Ability to stay upright when placed horizontally, and this design is also dependent on that the image sensor-board is free of obstacles at three of the sides.

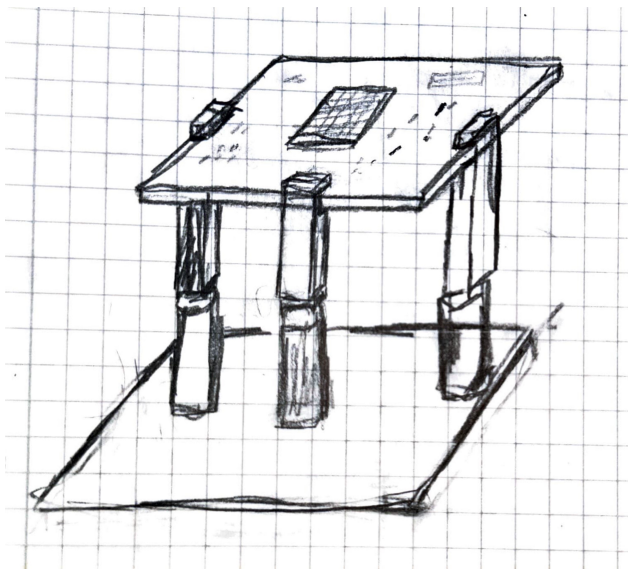

FIGURE 6.1: First sketch ever made of the prototype. Note the three piezoelectric stacks and the holders for the PCB on top.

A whole new approach was now used. After researching, see Chapter 2, it was found that the stacks are not susceptible to any shear stress, thus the idea of including "towers" for the stacks to sit in, in order to release them of any force, was drawn as seen in Figure 6.2.

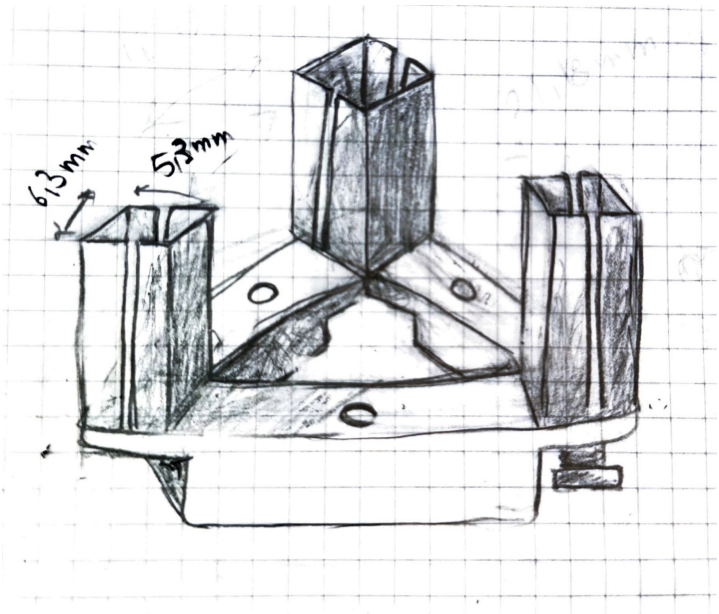

FIGURE 6.2: Another early stage sketch of the prototype.

As seen in the bottom right corner of the drawing, a screw was added under the actuator tower; This in order to manually adjust the height of the actuators in order to compensate for any individual height differences of the stacks, as stated in Table 4.1. This came to be a bigger problem than anticipated. The height adjusters must not rotate thus the actuators should be fastened with glue on the image sensor board. Another structure was also needed in order to hold the lens holder.

The following set-up, as shown in Figure 6.3, was then drawn. The sensor board was supported by springs to be held upwards and not put strain on the piezoelectric stacks. Two pins protruding from the lensholder were guided into holes on the sensor-PCB that also contributed to hold the structure upright and avoid putting shear stress on the stacks. A possible solution to the manual adjustment was drawn, however, it was decided that the prototype should be made without the manual adjustment to begin with.

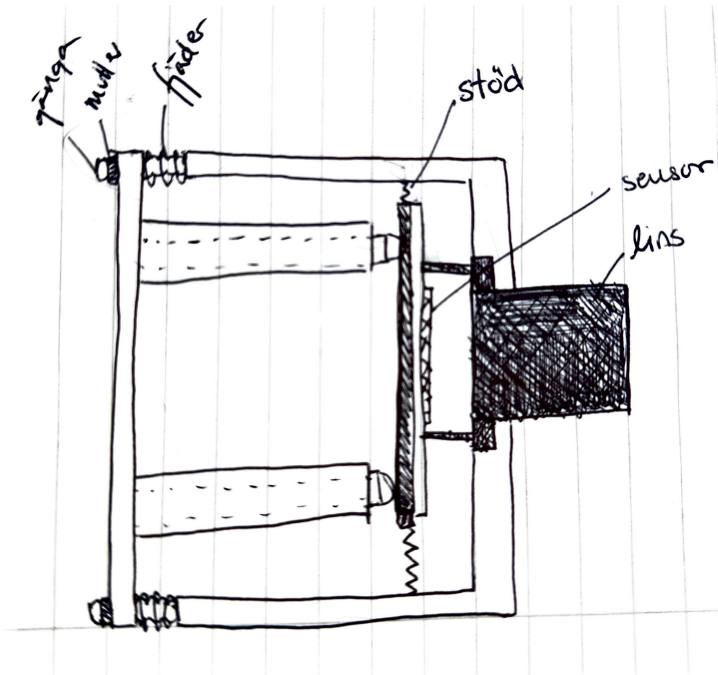

FIGURE 6.3: Sketch showing different options that could be used to counteract the shear stress on the actuators.

After taking the discussion from above into consideration, the following sketch, see Figure 6.4, was made.

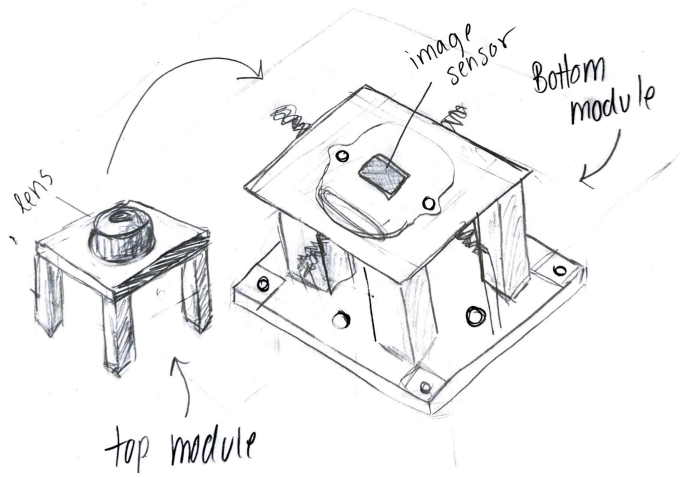

FIGURE 6.4: The last sketch before making a CAD drawing. It was decided to use two separate modules, one that holds the image sensor board using the piezoelectric stacks, and one that holds the lens.

After further consultations with a CAD-resource at the company, the design was further refined and made more compact, as seen in Figure 6.9.

6.2 Prototype 1

The prototype consists of four separate parts. The purpose of this was to make it possible for the image sensor to move, without disturbances, in relation to the lens. The bottom plate, as seen Figure 6.5, holds the three stacks which are glued into respective supporting structure. There are holes in the bottom of the plate to make room for, and minimize stress on, the cords from the piezoelectric stacks connection to the piezoelectric controllers.

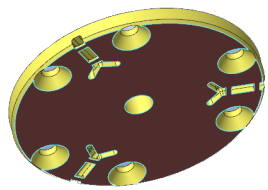

FIGURE 6.5: The base of the bottom plate where the actuators sit. Note the screw holes and the cut outs for the chords for each stack.

The top of the stacks are placed and glued into the upper support structures that holds the image sensor board, which can be seen in Figure 6.6. In this image, the former structure with long support structures are shown. This was later changed to much shorter structures as in Figure 6.10 since they only caused problems when trying to insert the actuators and did not give the support that was wanted.

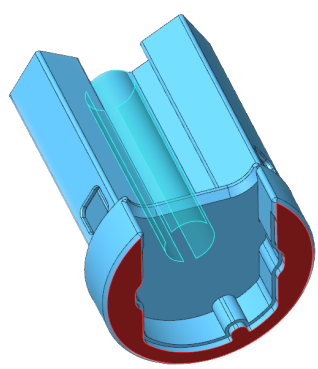

FIGURE 6.6: Image sensor board holder for M3065/85 camera. Note the long structures where the piezoelectric stacks would sit. This structure was shortened in another version of the prototype.

The top structure consists of only one 3D-printed piece and the lens which is glued to it. This piece has the same bottom diameter as the bottom plate and the two can be attached by screws. The top part has two small holes, as seen below in Figure 6.7 which matches the structure of the lens. These spikes from the lens also matches up with two holes in the image sensor PCB which allows for line up of the sensor with the lens with ease. This structure also has three legs that line up with the position of the piezoelectric stack as shown in figure 6.9.

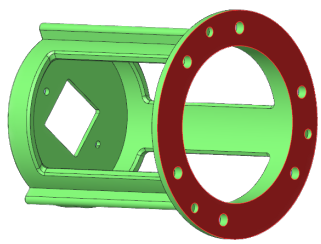

FIGURE 6.7: The lensholder with a cutout for the image sensor.

The large main board is attached to the mounting plate by screws and is parallel to the structure, see Figure 6.8 and Figure 6.9.

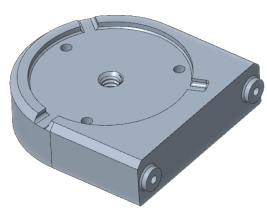

FIGURE 6.8: Mounting plate for the whole structure. The screw holes on the side holds the large PCB.

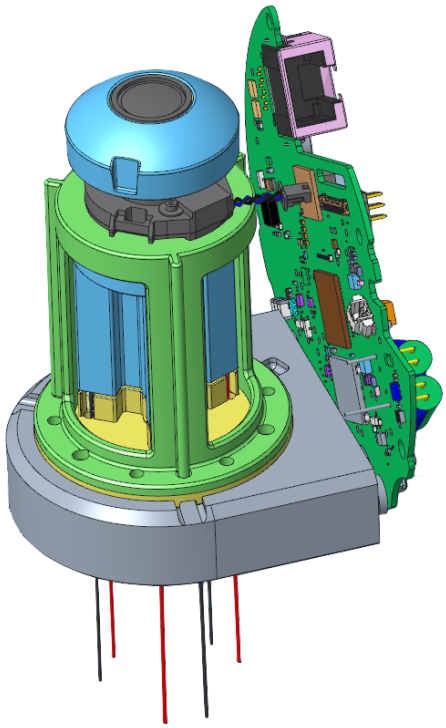

FIGURE 6.9: The complete set-up for the M3065/85 camera. Note the structures surrounding the stacks that was not used.

6.2.1 Change of Camera

It was decided that a change of camera was necessary after conducting a few tests due to the current camera only having 2 MP and a higher number of pixels would show a greater sensitivity to focus change. Being that there was no desire to remodel the whole prototype and possibly using an entirely different type of camera with another type of optics and sensors to take advantage of their extreme sensitivity, a camera within the same category was chosen: The new M3088 with 8 MP and 4K resolution.

6.3 Prototype 2

Most of the first prototype design was used in the second, only the opening for the image sensor board in the image sensor board holder as well as the lensholder was adjusted to fit the new camera and lens, see Figures 6.12 a) and b). The final CAD-model for prototype 2 can be seen in Figure 6.10.

As mentioned, the long support structures in Figure 6.6 were shortened down and the final prototype is shown in Figures 6.10 **??** a) and b).

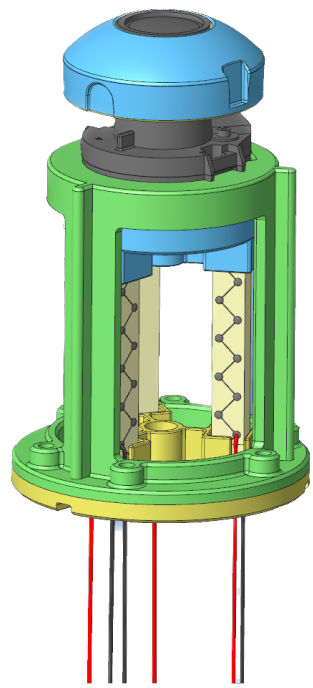

FIGURE 6.10: The final prototype with the M3088 camera without the mounting plate. Note that the support structure for the piezoelectric stacks are shortened.

a)

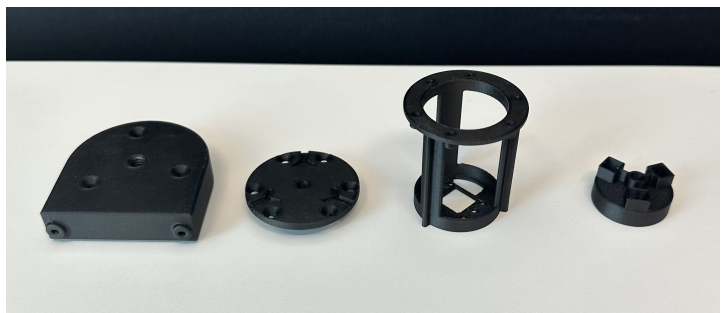

b)

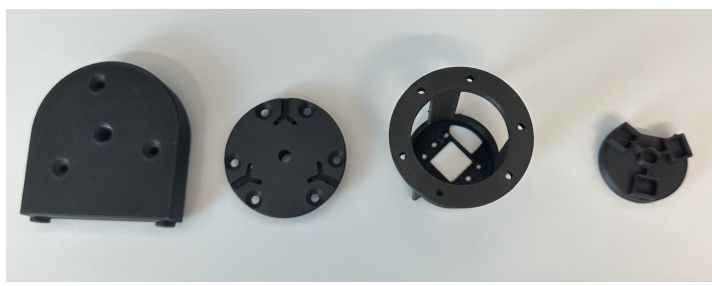

FIGURE 6.11: The final prototype parts printed out using a 3D printer.

a)

b)

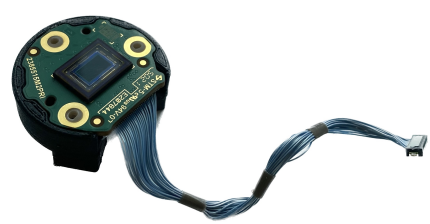

FIGURE 6.12: The image sensor board holder with and without the board in. a) shows the board holder, and b) shows the board holder with the board in it.

Following, in Figure 6.13, shows the prototype half assembled with only the stacks and sensor attached. Here it can be noted that the design is made so that the actuators can move the sensor freely.

a) 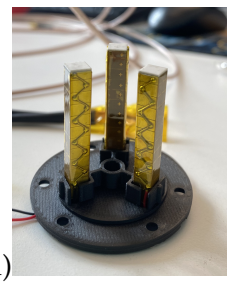 b) 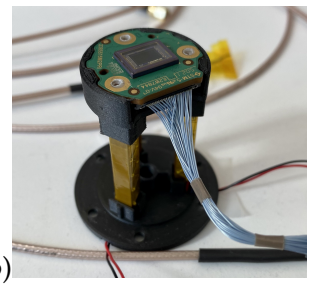

FIGURE 6.13: The 3D printed parts attached to the piezoelectric stacks. The picture in a) represents the stacks placed in their holder with the board holder placed on top. The picture in b) represents the stacks placed in their holder.

Below, in Figure 6.14, the full printed prototype is shown, without anything attached. The bumps on the top makes for a greater alignment with the lens and ensuring the distance to the sensor is optimal.

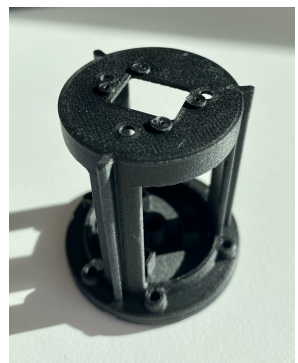

FIGURE 6.14: The 3D printed lensholder-structure. Note the protruding structures around the sensor-cutout that establish the correct distance between the lens and sensor.

6.4 Tilt

By applying voltage to the piezoelectric stacks the image sensor can be moved up and down, and due to there being three stacks, the sensor can be tilted. The placement of the piezoelectric stacks in relation to each other can be seen in Figure 6.15.

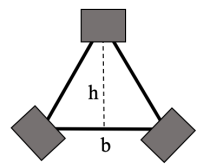

FIGURE 6.15: The placement of the three piezoelectric stacks.

The distance between each stack is of approximately 18 mm measured from the middle of each stack. The height of the triangle is:

$$tan(60) \cdot \frac{18}{2} = 15.6mm \tag{6.1}$$

The maximal angle of tilt that can be created with this prototype is when two stacks are fully extended and the third not extended at all, for example the top stack is not extended but both bottom stacks are, see Figure 6.17 a). This was referred to as "backtilt" and the opposite "fronttilt", see Figure 6.16.

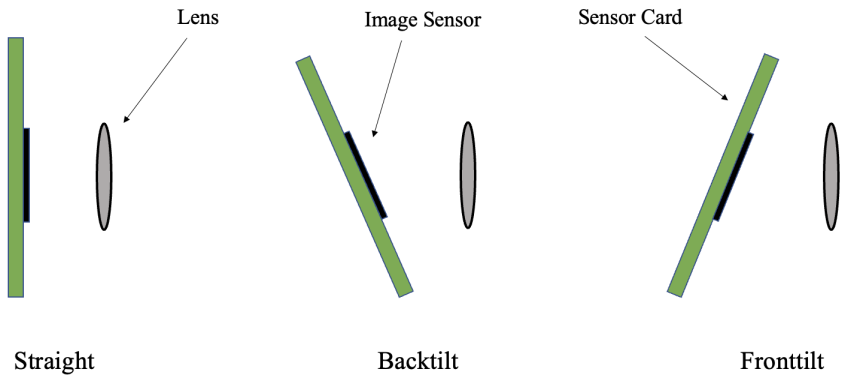

FIGURE 6.16: Schematic representation of the sensor board being tilted by the pressure of the piezoelectric stacks.

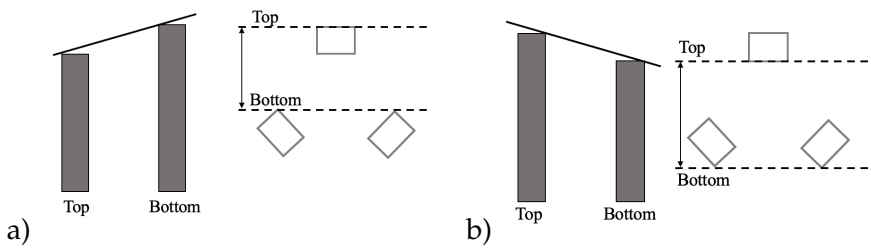

FIGURE 6.17: a) The piezoelectric stacks from the side when the two bottom stacks are fully extended. The black line is the sensor board. The second image shows the stacks seen from above. The dotted lines mark the limiting edges where the sensor board is supported by the stacks. b) Same as in a) but when the top stack is fully extended.

The way the prototype is constructed creates a difference in length if one or two stacks is extended, compare the distances marked with an arrows in Figure 6.17. When measuring the distance in a) is 14 mm and 17 mm in b).

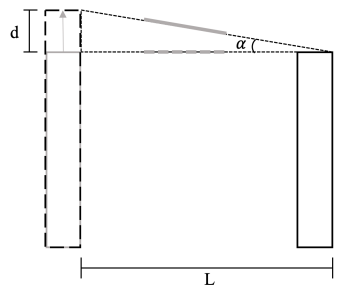

FIGURE 6.18: The piezoelectric stacks seen from the side, when the dotted stack is fully extended. The distance L is the distance between the two limiting edges of the stacks. The distance d is the displacement. The angle α is the amount of tilt. The grey piece in between the stacks marks approximately where the sensor sits on the sensor board.

If the displacement of the top stack is 41 μm, the two bottom stacks has a 0 μm displacement and the length L is 17 mm the angle α is:

$$arctan(\frac{41 \cdot 10^{-6}}{17 \cdot 10^{-3}}) = 0.138^{\circ} \tag{6.2}$$

The same calculation for L = 14 μm gives a tilt of 0.168 $^{\circ}$. However, even though this will be the tilt of the sensor the top of the sensor will not move the full length of the displacement. This is due to the fact that the distance between the stacks is larger than the size of the sensor and the point of rotation does not necessarily lay on the sensor, but moves around depending on the different displacements. This also means the entire sensor will move upwards, see Figure 6.19.

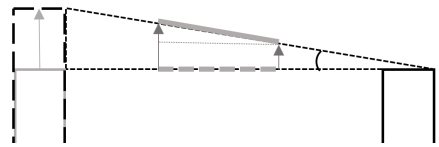

FIGURE 6.19: The sensor (grey) will not move the entire distance of the displacement from the extended piezoelectric stack.

The piezoelectric stacks are sensitive to stress. If the entire top of stacks if flat against the sensor board and the board is tilted a force arises on each stack to counter the tilt, see Figure 6.20

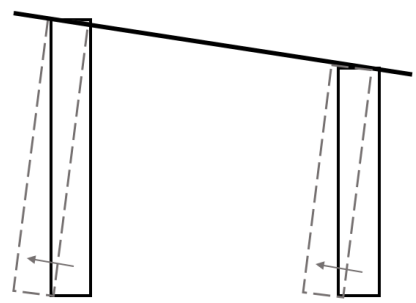

FIGURE 6.20: When the sensor board is tilted a strain will be put on to the piezoelectric to move. The movement is illustrated by the arrows and dotted piezoelectric stack.

As a first prototype it was assumed that the small angle would not be enough to make the strain a concern. Instead a rubber based super glue: Super Glue Power Gel from Loctite was used in order to have a strong but flexible hold. If a prototype was constructed to be able to have a larger tilt the strain may be a problem. One solution would be to have piezoelectric stacks with an end hemisphere and a matching end cup attached on the base of the sensor board structure, see Figure 6.21. This would work as a socket joint and allow the sensor board

to tilt without putting stress onto the stacks. However, with such a structure one should make sure not to introduce any extra looseness, which the more "free" movement could create. Each small unwanted movement could be problematic.

FIGURE 6.21: A piezoelectric stack with an end hemisphere from Thorlabs [24].

As the size of the tilted angle depends on the distance between the stacks as well as the size of the displacement, if a larger tilt is desired one or both of these two factors should change.

Chapter 7

Auto Focus Algorithm

7.1 Background

When the previous experiments were preformed, the stacks were controlled manually by using the user interface provided by Thorlabs. Even though this worked in the given conditions it would be hard to achieve the optimal focus by hand. The shift in focus was observed by comparing images by eye, which is not quantifiable. By using an algorithm to control the piezoelectric stacks, the goal was to achieve a better focus value quicker and with better precision. The amount of shift in focus would also be quantified and therefore also measurable. To create an algorithm specifically to control the tilt of the sensor also became of desire, as the individual movement of the piezoelectric stacks affect the movement in a more complicated manner than compared to up and down.

7.2 The Algorithm

Thorlabs provide a software, Kinesis®, with an easy to understand user interface where each controller manually connects, is enabled and can provide a chosen voltage. Kinesis® has a .NET control feature where third-party developers can create their own custom applications using any programming languages compatible with .NET. The .NET package was downloaded from Thorlabs website and used in the Python code. The code is in Appendix A.

In this project, the programming language of choice was Python. The code to connect the controllers to the computer using Python was provided by Thorlabs via their GitHub [28] and a toolbox of methods were found in the .NET package. The code was then altered to fit the specific needs for this set-up by integrating it with code that takes an image from the camera and then calculates the focus value in the center and three regions of the image, as seen in Figure 5.5. The three regions corresponds to the approximate placements of the piezoelectric stacks behind the image sensor in order to make the tilt easier to perceive.

7.2.1 Structure of the Code

Two classes were made: Camera and Device, which each makes one able to creates a camera and device object. A device object creates a connection to a piezo controller by inputting the controller serial number. A few of the methods created includes: setVoltage(Voltage), which sets a specific voltage to the controller which consequently puts a displacement on the piezoelectric stack. Another example is the method disconnectDevice() which sets the voltage to zero and disables the controllers.

The camera class creates a connection to the camera based on its IP-address, thereby enabling the retrieval of live images that can be saved using: getImage() that returns the image at that point in time. The methods getCenterfocus value(image) and getCornerfocus value(image, nbr) calculates the focus value for the center and for the corner corresponding to the device which is given as the input. As discussed in Chapter 5, each ROI, as seen in Figure 5.5, that is used for calculating the focus value approximately corresponds to the placement of piezoelectric stacks. This was done in order to make tilting easier.

7.2.2 The Algorithm in Words

The focus algorithm works in the following way:

- Takes an image and calculate the initial focus values in all of the ROI and save the values.

- Repeat previous step for voltages 0-150 V with increments of 5 V.
- Search for the voltage corresponding to the highest focus value for the center region.
- Set each stack to that voltage.
- Find the corner region with the lowest focus value in order to enhance the focus in the corresponding corner.
- Traverse the device corresponding to that corner region through 0-150 V with increments of 5 V and save the focus values.
- Find the voltage with the highest focus value for the corner with the lowest initial value.
- Set that device to that voltage.

7.2.3 The Focus Value

Firstly, a gray scale image is made out of the original image in the ROI's as seen in Figure 5.5. Then a Laplacian operator is applied to the same areas; The standard one in the library on the Python platform: "OpenCV" is a negative kernel. This highlights the regions of rapid intensity change. Finally, the variance of the filtered image is calculated.

Chapter 8

Results & Discussion

8.1 HIT Corner Focus-Measurements

8.1.1 M3085/65 - Manual

During these tests one key insight was discovered; Depending on where the focus is initialised, which is changed by moving the lens manually by rotating it in its thread before moving, a difference in amount of focus shift was achieved. I.e, if the focus was manually placed at the top of the focus-graph (best possible focus) very little would happen to the focus, both when looking at an image or by studying the values. This could be due to the f-number of the lens used which affect the width of the peak. If the peak is too wide for the 41 μm displacement of the stacks, a shift in focus will be hard to detect with the naked eye when the focus value is high, i.e being on top of the peak. What was done was that the focus was strategically put at the value 60-70 (different for each corner) and then making the image better by moving the stacks closer to the lens, then resetting the position of the stacks, changing the focus manually to a value of 90-100 at the "other side" of the curve for the next test and thus making the image worse by and once again moving the stacks towards the lens to get a negative slope.

One aspect that is prominent in all figures in Chapter 8 is the fact that all corner and center focus values tend to begin and end at different points, as well as acting quite differently. Being that both the HIT

corner focus test and the Python auto focus algorithm are very sensitive to changes, there are many contributing factors that could explain this behaviour. Firstly, from Table 4.1, where the specifications of the piezoelectric stacks are listed, one can gather that the stacks have an individuality of $\pm$ 0.1 mm = 100 μm, which is more than the displacement of the stacks. This means that, unless compensated for when building the prototype, which could not be achieved in this project, the prototype might have an inherent tilting of the sensor board in the structure already. This will produce different graphs for each corner. Secondly, when gluing the stacks to the bottom and top structure, the amount of glue, and the way the stacks are placed in this glue, may also contribute to errors that can be observed in the graphs below. Finally, the slightest of changes in the targets of the ROI such as the amount of illumination, size and placement of the Siemens stars and background of the Siemens stars will alter the results. If one corner is, for example, exposed to more light than another, this will be noticeable in the graphs. By conducting most test in a controlled environment, as was done in this thesis, this margin of error could be reduced.

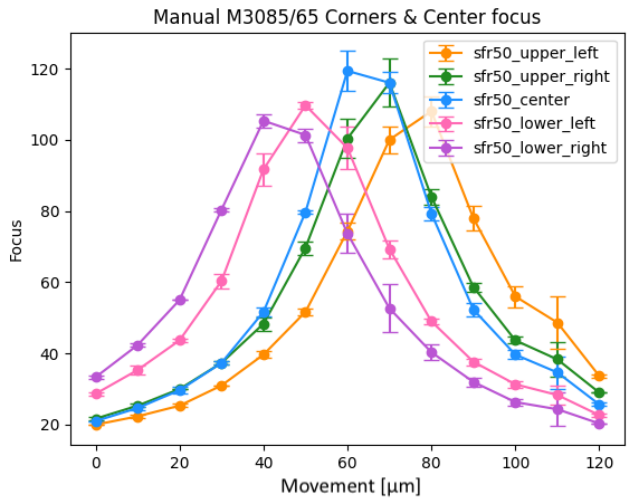

FIGURE 8.1: The plot of the corner focus test of the manual set-up of the M3085/M3065 camera. The standard deviation is also plotted. For example upper left corresponds to the upper left corner in the image.

The measurement from the manual set-up of the M3085/65 camera, see Figure 8.1, is a second degree equation curve. As the focus value increases the image quality increases. This is the result of the mean value of three separate measurement. The thickness of the peak determines how sensitive the set-up is to movement of the sensor in relation to the lens. In production a camera could for instance have good enough focus if the value is 70 or above. If this where the case these measurements would give a span of "good focus" around 30 μm.

8.1.2 M3085/65 - Prototype

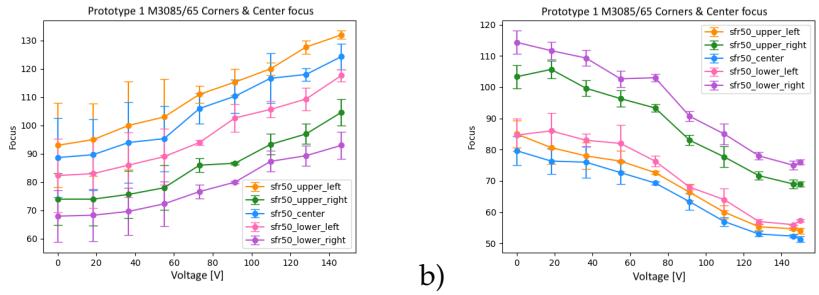

FIGURE 8.2: The plot of the corner focus test of the first prototype with the M3085/M3065 camera. The standard deviation is also plotted. In a) a better focus value is achieved when the voltage is increased. In b) a better value is achieved when the voltage is low. The standard deviation is also plotted.

The measurements of the prototype 1 is also the mean value of three separate measurements, see Figure 8.2. If the measurements of the prototype is compared to the measurement of the manual set-up, it is possible to see that it follows the same pattern. When the starting value is in front of the peak value the value increases, see Figure 8.2 a) and when the staring value is after the peak value the values decreases, Figure 8.2 b).

However, it might not be fair to compare the two measurements more specific as the focus value are very sensitive to all type of change. The two set-upswere at similar placement in relation to the target, however the placement was not exact. Even though the same model of camera was used, different set of lenses and sensors where used. As the individual property of each lens or sensor may affect the appearance of the curve. Even to compare the two curves in Figure 8.2 may be misleading as the starting point in focus was changed manually between the two tests. In other words, the lens was moved by hand and even though the lens is glued to the top of the prototype the lens component itself is "free" in its thread. Due to the clearance between

the lens and its thread the lens will probably have moved in both z, x and y- direction.

How much the value increases as the movement increases depends heavily on where on the focus curve the starting value is. However these result strongly suggest that the piezoelectric stacks moves as expected.

8.1.3 M3088 - Manual

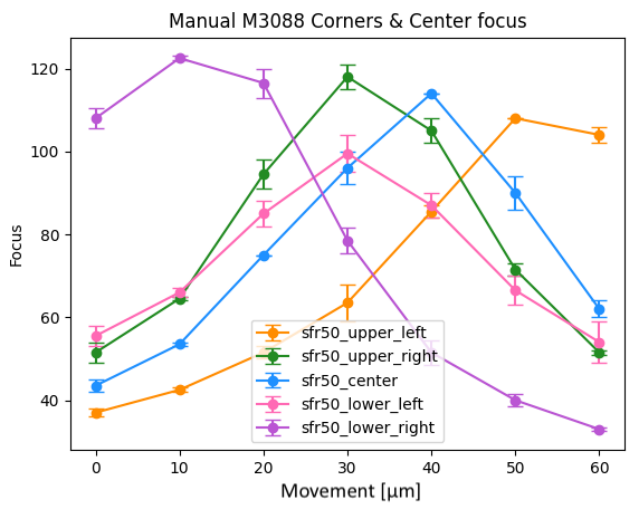

FIGURE 8.3: The plot of the corner focus test of the manual set-up of the M3088 camera. The standard deviation is also plotted.

8.1.4 M3088 - Prototype

a)

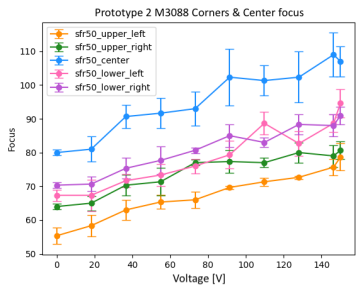

b)

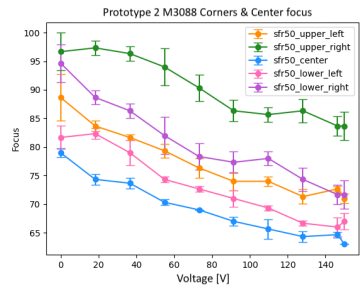

FIGURE 8.4: The plot of the corner focus test of the manual set-up of the M3088 camera. The standard deviation is also plotted. In a) a better focus value is achieved when the voltage is increased. In b) a better value is achieved when the voltage is low. The standard deviation is also plotted.

In Figure 8.3 the plot of the corner focus test for the manual set-up of the M3088 can be seen. The size of the x-axis is limited to the extent that the test could produce a successful value. The large spread and differences in the different center and corner, shows the difficulty of aligning the sensor in relation to the lens. In the Figure 8.4 the corner focus test for the M3088 prototype 2 set-up can be seen. The same overall discussion can be held for these to set-up as for the manual set-up of M3085/65 and prototype 1.

8.2 Image Comparisons

8.2.1 M3065/85 - Prototype

Figures 8.5, - Figure 8.8 displays one of the first images taken with the first prototype. The images are taken of the whiteboard in the office space with Siemens stars attached in order to study the differences with 0 V and 150 V.

a)

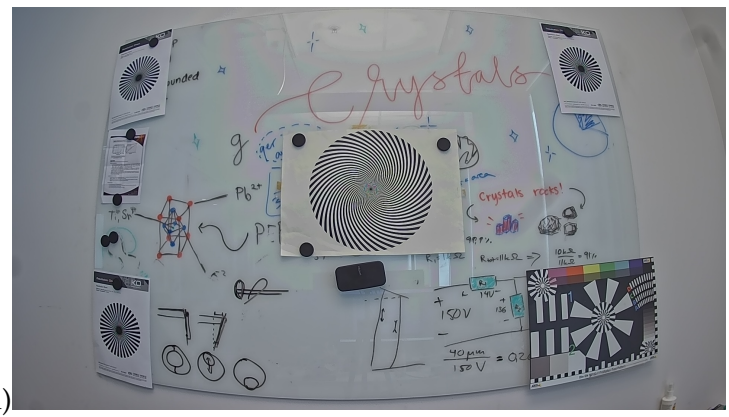

b)

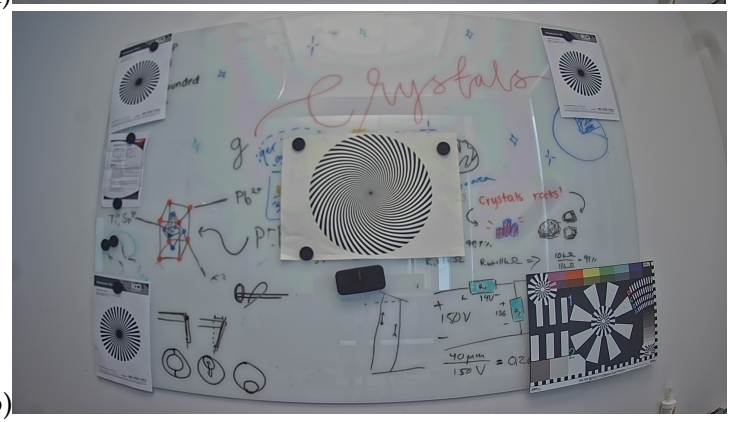

FIGURE 8.5: Images of whiteboard with Siemens stars. a) displays the image when the piezoelectric stacks have a voltage of 0 V. b) displays the image when the piezoelectric stacks have a voltage of 150 V.

a) 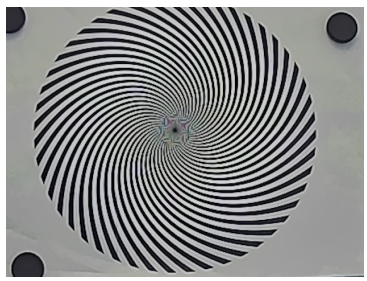 b) 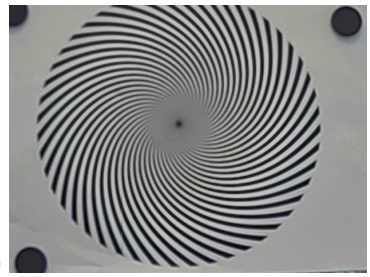

FIGURE 8.6: Zoomed in images of the center of the whiteboard. a) displays the image when the piezoelectric stacks have a voltage of 0 V. b) displays the image when the piezoelectric stacks have a voltage of 150 V.

a) b) 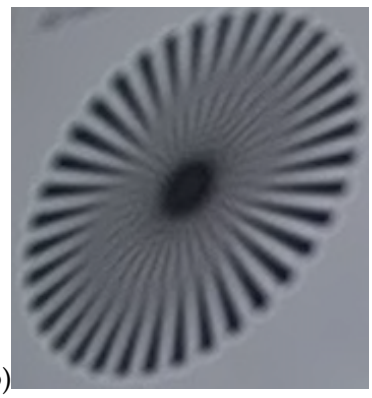

FIGURE 8.7: Zoomed in images of the left corner of the whiteboard. a) displays the image when the piezoelectric stacks have a voltage of 0 V. b) displays the image when the piezoelectric stacks have a voltage of 150 V.

a) 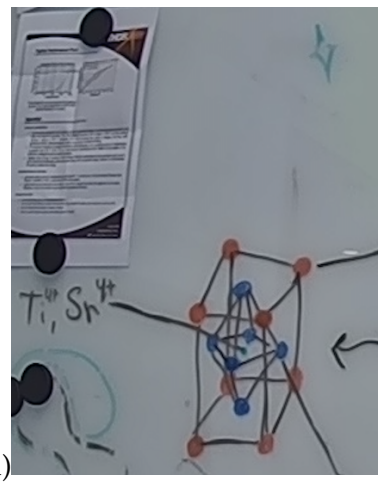 b) 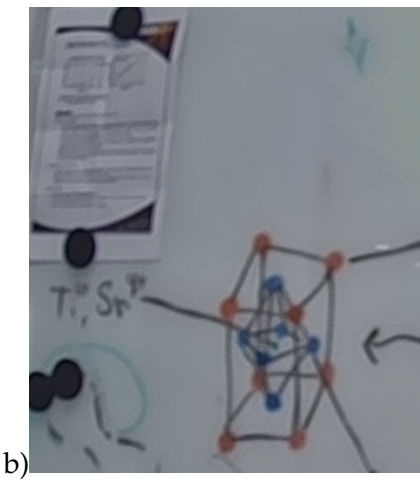

FIGURE 8.8: Zoomed in images of scribbles on the whiteboard. a) displays the image when the piezoelectric stacks have a voltage of 0 V. b) displays the image when the piezoelectric stacks have a voltage of 150 V.

As seen in the figures above, the technology provides for prominent changes in the amount of focus.

8.2.2 Comparisons with the Manual set-up

M3085/65 - Manual Test 1

a) b) 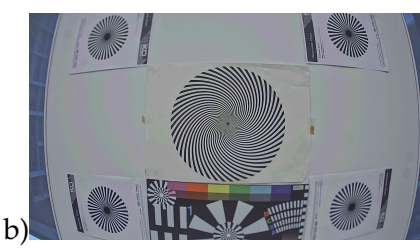

FIGURE 8.9: Manual set-up of the M3085/65 camera. (a 0 μm (b Sensor moved 41μm away from the lens.

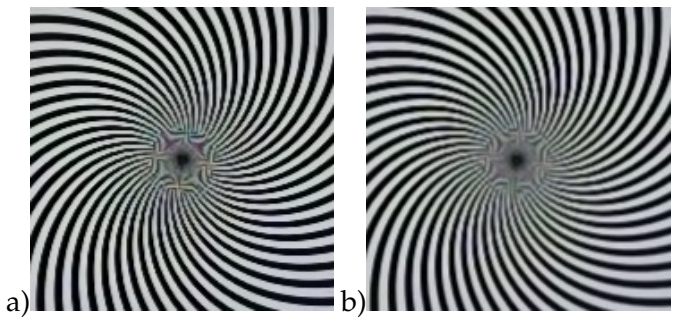

FIGURE 8.10: Manual set-up of the M3085/65 camera. a) Center of image 0 μm away from the starting point. b) 41 μm away from the starting point.

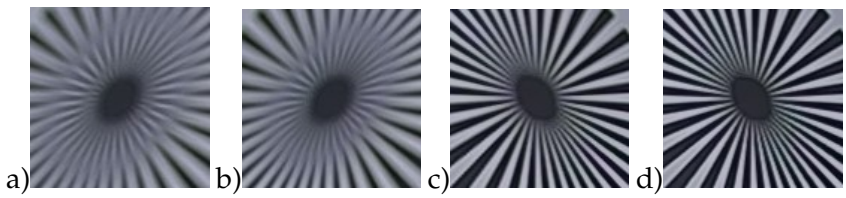

FIGURE 8.11: Manual set-up of the M3085/65 camera. a) Left upper corner of image 0 μm b) Left upper corner of image moved 41 μm away from the lens. c) Right upper corner of image 0 μm d) Right upper corner of image moved 41 μm away from the lens

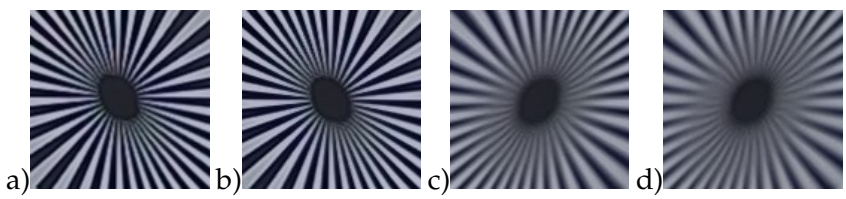

FIGURE 8.12: Manual set-up of the M3085/65 camera. a) Left upper corner of image 0 μm b) Left upper corner of image moved 41 μm away from the starting point. c) Right upper corner of image 0 μm d) Right upper corner of image moved 41 μm away from the starting point.

See discussion of test 1 to test 2 in the paragraph below.

M3085/65 - Manual Test 2

a) b)

FIGURE 8.13: Manual set-up of the M3085/65 camera. (a 0 μm (b Sensor moved 41 μm away from the starting point.

a) b) 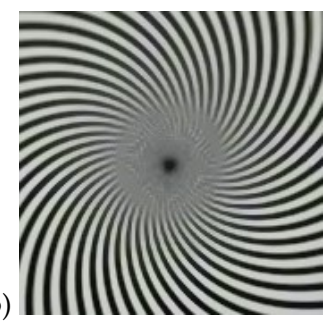

FIGURE 8.14: Manual set-up of the M3085/65 camera. a) Center of image 0 μm away from the starting point. b) Center of image 40 μm away from the starting point.

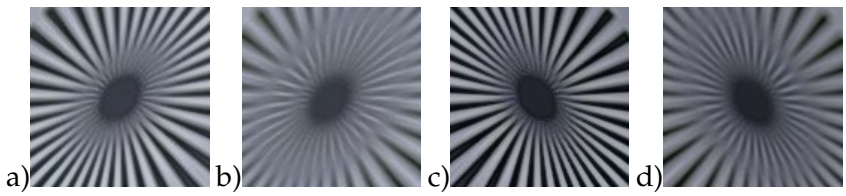

FIGURE 8.15: Manual set-up of the M3085/65 camera. a) Left upper corner of image 0 μm b) Left upper corner of image moved 41 μm away from the starting point. c) Right upper corner of image 0 μm d) Right upper corner of image moved 41 μm away from the starting point.

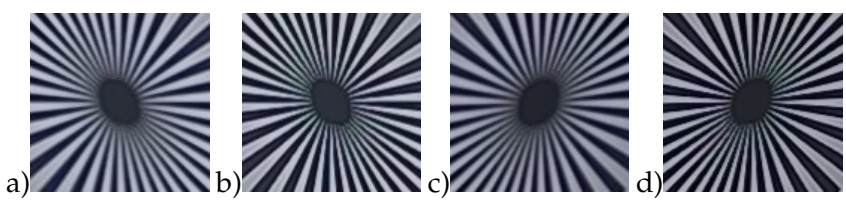

FIGURE 8.16: Manual set-up of the M3085/65 camera. a) Left lower corner of image 0 μm b) Left lower corner of image moved 41 μm away from the starting point. c) Right lower corner of image 0 μm d) Right lower corner of image moved 41 μm away from the starting point.

Comparing the images from M3085/65 - Test 1 images 8.9 - 8.12 and M3085/65 - Test 2 images 8.13 - 8.16 it is possible to see a large difference in the amount of focus shift even through the set-up and the total distance the sensor was moved were the same amount. The only thing different from the two is that the focus of the first image was shifted. This means that the focus value was probably lower to start with in test 2 in Figure 8.13 than in test 1 in Figure 8.9 so the movement of 41 μm gave a larger shift in focus, as the focus value follows a second degree function, see Figure 8.1. This further proves the uncertainty to compare images where the starting focus has been altered, as the amount of shift of focus depends both on the moved distance of the sensor as well as the amount of focus on the staring image.

M3088 - Manual Window Test

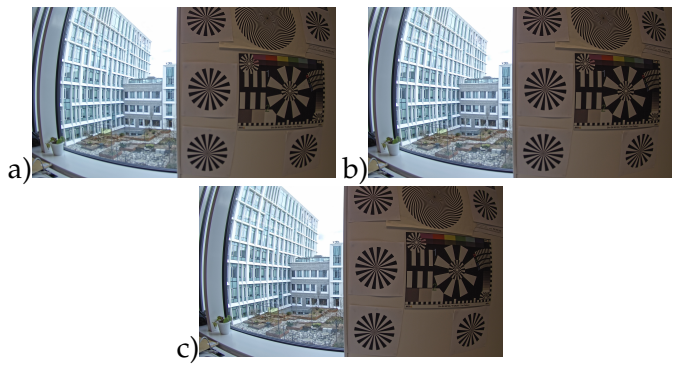

FIGURE 8.17: Manual set-up of the M3088 camera. a) 0 μm b) 20 μm c) 40 μm.

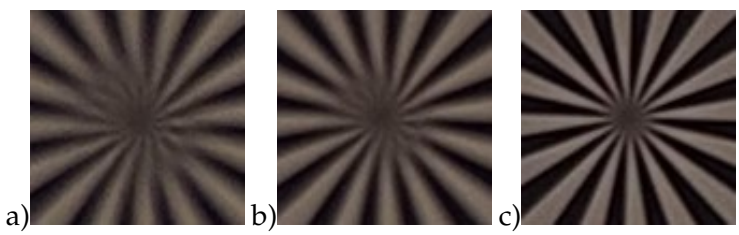

FIGURE 8.18: Manual set-up of the M3088 camera. Super close up of center of a siemens star. a) 0 μm b) 20 μm c) 40 μm

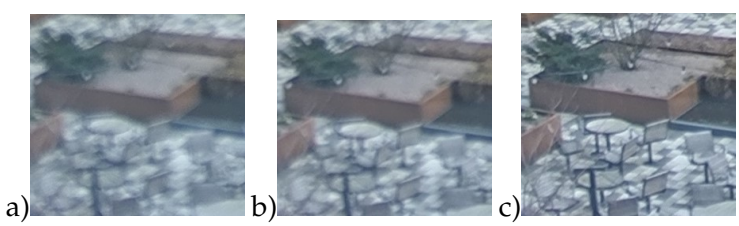

FIGURE 8.19: Manual set-up of the M3088 camera. Close up of chairs at a far distance. a) 0 μm b) 20 μm c) 40 μm

Images in Figure 8.18 and Figure 8.19 is close-ups of the image in Figure 8.17 showing Siemens stars close to the camera as well as a more distant view out a window. This was the manual set-up with the M3088 camera. The 0 μm image is the starting point and 20 μm and 40 μm is the distance the image sensor has moved towards the lens. As the sensor board moves closer to the lens the image quality improves in these set of images. The series of images show that a displacement of 41 μm is enough to see a clear difference in image quality.

M3088 - Prototype Window Test

a) 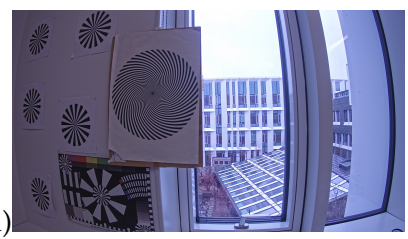 b)

FIGURE 8.20: Images taken using Prototype 2. The image in a) is taken at 0 V and in b) at 150V.

a) 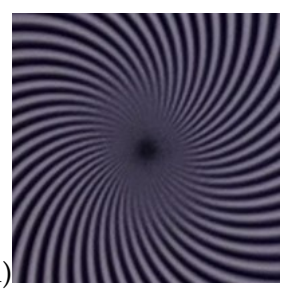 b) 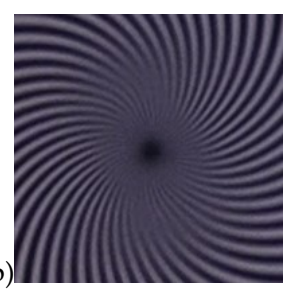

FIGURE 8.21: Zoomed in mages taken using Prototype 2. The image in a) is taken at 0 V and in b) at 150V.

a) b) 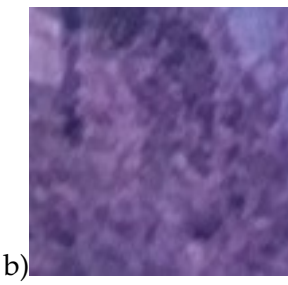

FIGURE 8.22: Zoomed in mages taken using Prototype 2. The image in a) is taken at 0 V and in b) at 150V.

a) 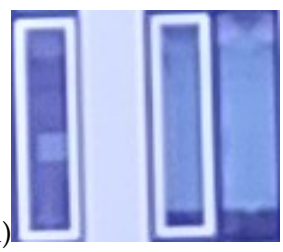 b) 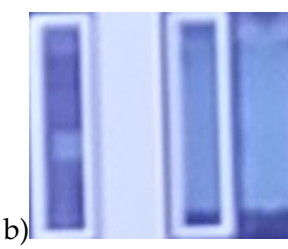

FIGURE 8.23: Zoomed in mages taken using Prototype 2. The image in a) is taken at 0 V and in b) at 150V.

Images in Figures 8.21 - Figure 8.23 are close ups of the image in Figure 8.20 showing Siemens stars close to the camera as well as a more distant view out a window. This was the set-up of prototype 2. The first image 0V is the starting point and second is when 150 V is applied over the piezoelectric stacks, corresponding to 41 μm. The series of images show that a movement/displacement of 41 μm is enough to see a difference in image quality.

If compared to the image in Figure 8.17 taken by the manual set-up, there might not be as clear shift in quality change. As discussed in the beginning of Chapter 8 this may depend on a multiple of reasons, for example where on the focus curve the focus is, that the view is out of two different windows, taken in two different days which affect the distance to the objects in the images as well as the brightness. The

size of the close up is also not the same. Additionally, it can not be ruled out that the piezoelectric stacks in the prototype does not move the full 41 μm, for example due to its uncertainty of the displacement size, see Table 4.1.

8.2.3 Close and Far Distances within the Same Image - Hallway

a) b)

FIGURE 8.24: An image of a hallway taken with the M3088 Prototype 2. The voltage across the piezoelectric stacks were a) 0 V and b) 150V.

a) b) 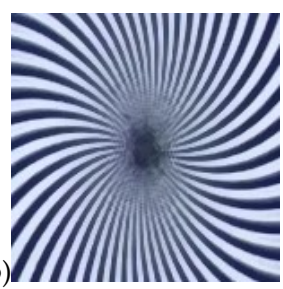

FIGURE 8.25: Close up of a the Siemens star close to the camera in Figure 8.24 Taken with m3088 Prototype 2. The voltage was a) 0 V b) 150V

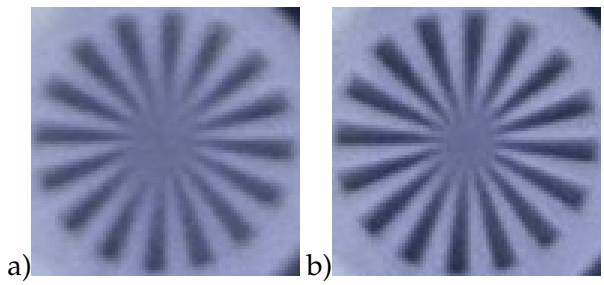

FIGURE 8.26: Close up of a the Siemens further away from the camera in Figure 8.24 Taken with m3088 Prototype 2. The voltage was a) 0 V b) 150V

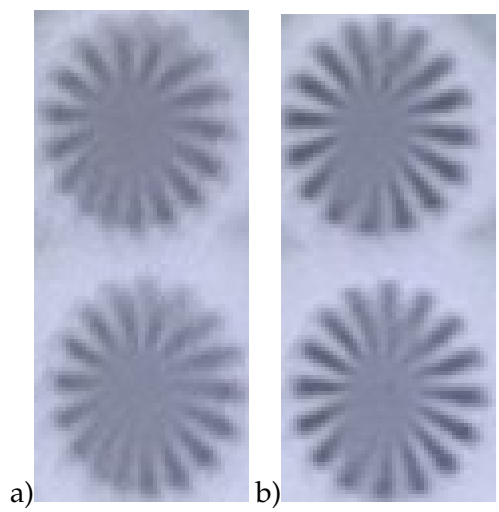

FIGURE 8.27: Close up of a the Siemens star furthest away from the camera in Figure 8.24 Taken with m3088 Prototype 2. The voltage was a) 0 V b) 150V

When studying the images in Figure 8.24 it is possible to seen that the focus close to the camera does not change much, see Figure 8.25. However, the focus of the Siemens star at a further distance is improved when the 150 V is applied across the piezoelectric stacks, see Figure 8.26. The Siemens stars furthest from the camera is also improved at 150 V, see Figure 8.27

A Person at Different Distances

FIGURE 8.28: A person at a distance of 18m away from the camera. The image is taken by the M3088 prototype 2. Close up can be seen in 8.31.

FIGURE 8.29: A person at a distance of 6m away from the camera. The image is taken by the M3088 prototype 2. Close up can be seen in 8.32.

FIGURE 8.30: A person at a distance of 3m away from the camera. The image is taken by the M3088 prototype 2. Close up can be seen in 8.33.

a) b)

FIGURE 8.31: Close up taken by the M3088 prototype 2 at a) 0 V and b) 150V. The full image of a) can be seen in Figure 8.28

a) 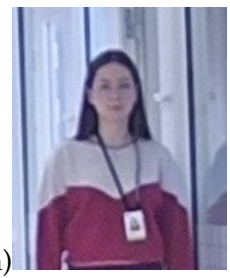 b) 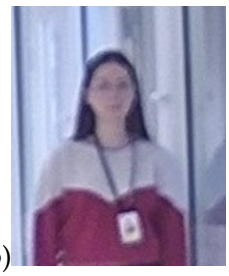

FIGURE 8.32: Close up taken by the M3088 prototype 2 at a) 0 V and b) 150V. The full image of a) can be seen in Figure 8.29

a) 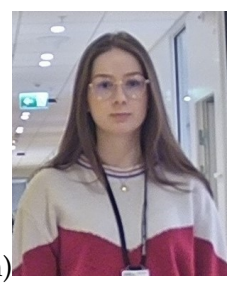 b) 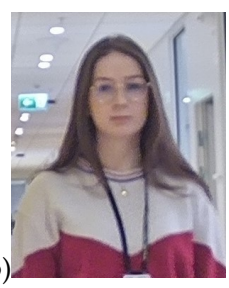

FIGURE 8.33: Close up taken by the M3088 prototype 2 at a) 0 V and b) 150V. The full image of a) can be seen in Figure 8.30

By comparing the images in Figure 8.28 - Figure 8.33 with and without a voltage over the prototype it is possible to see a difference in sharpness in the images. This proves a movement of the piezoelectric stacks which result in a movement of the image sensor. When a person is at a further distance the amount of movement is enough to make the face difficult to recognise with this type of camera, see Figure 8.32. Note that the focus was manually shifted between each image.

8.3 Focus algorithm

The following section displays the graphs and images obtained from running the written code on the prototype, meaning the focus value is

now calculated differently than in the HIT-tests, see Chapter 6 about "Focus Algorithm".

8.3.1 Hysteresis

By measuring the focus value in different images when incrementally varying the voltage within the range of 0 V to 150 V and then back one gets the graph in figure 8.34. This graph clearly depicts the hysteresis in the piezoelectric stacks.

The manufacturer of the piezoelectric stacks claim the piezoelectric stacks have a hysteresis of about +/- 15 %, as seen in Table 4.1. From Figure 8.34 below, the hysteresis is measured to be about 40%. The manufacturer measure the hysteresis based on its displacement, as in Figure 4.2. However, here it is measured based on the focus value from the written algorithm, and therefore there are more factors that can affect the hysteresis, than only the displacement.

When looking at the graph the similar shape between the up and down curve suggests that the time it takes to discharge the piezoelectric stacks might be affecting the result. Meaning that the stacks have a higher voltage then the controllers are supplying. However, in the code used (see Appendix A) a sleep of 5 seconds was put after the change of voltage, to make sure the stacks had time to discharge. The measurement in Figure 8.46, where a probe was used to measure the discharge time, showed a discharge time about 90ms when going from 150 V to 0 V. This suggest that the sleep of 5 seconds should be plenty of time to adjust to the new voltage.

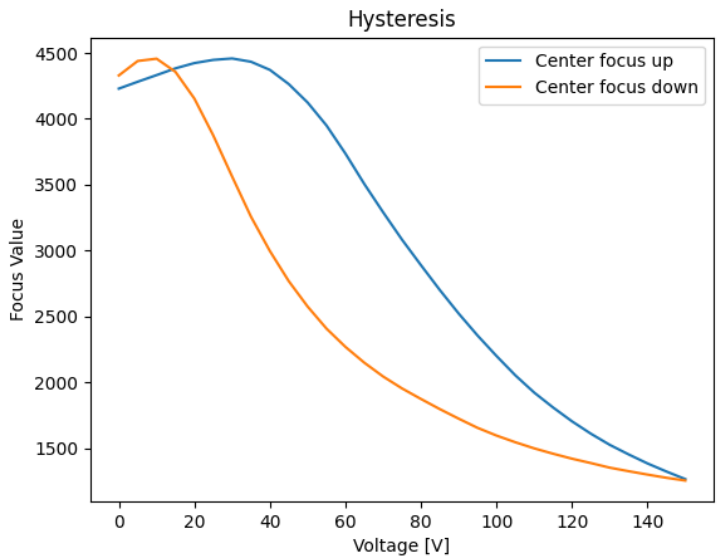

FIGURE 8.34: Graph showing the hysteresis in the piezoelectric stacks captured in the focus values of the images taken from 0-150V with steps of 5V.

8.3.2 Running the Algorithm

By running the algorithm over the whole voltage-range with increments of five volts the graphs in Figures 8.35, 8.39 and 8.42 were achieved. By studying these graphs and their images in Figures 8.36, 8.40 and zoomed in, in Figures 8.37, 8.38, and 8.41, one can clearly notice a difference in the amount of focus. In the first figures one notice a worsening of the quality and in the latter images, an improvement can be studied.

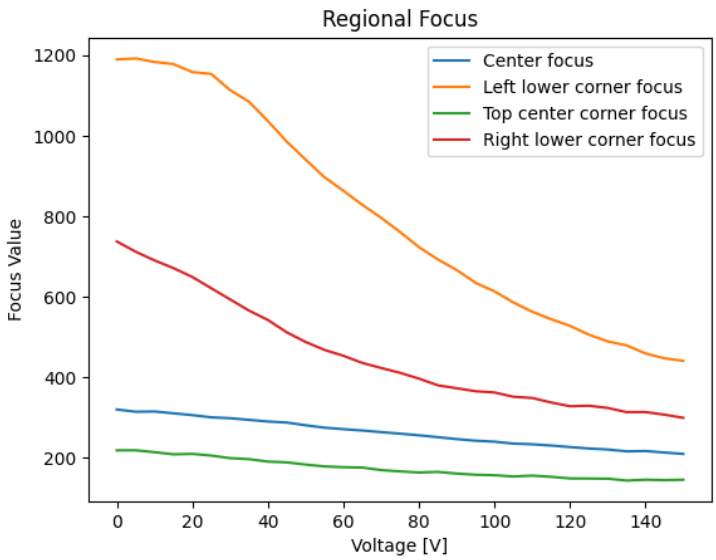

FIGURE 8.35: Graph depicting a worsening in the focus of the image when applying a voltage to the stacks. Note the yellow line (Left lower corner), having the biggest change of focus.

a)
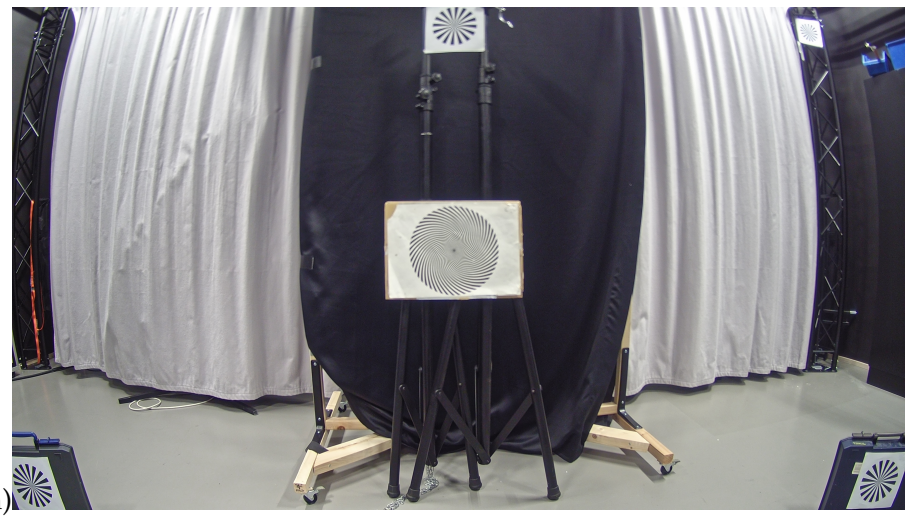

b)
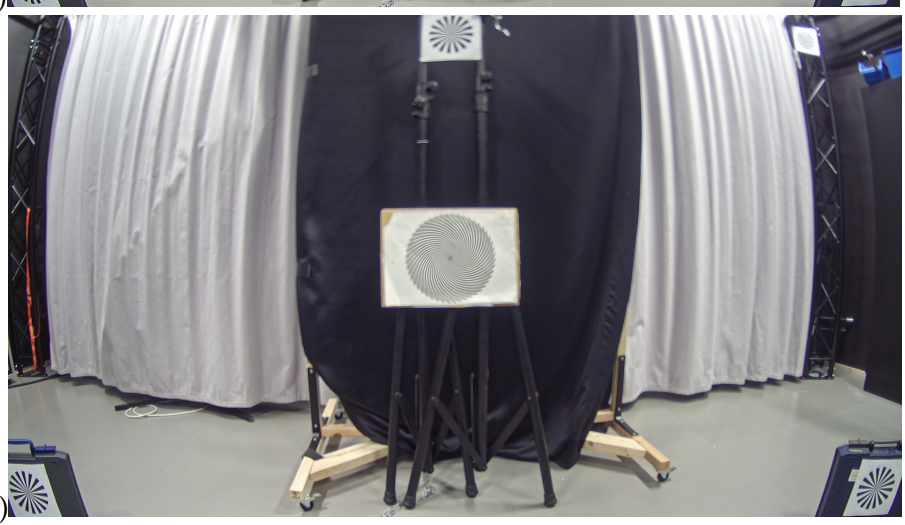

FIGURE 8.36: Images at a) 0 V on all the piezoelectric stacks, and b) 150V on all the stacks. Note the worsening of the quality in the latter image.

a) 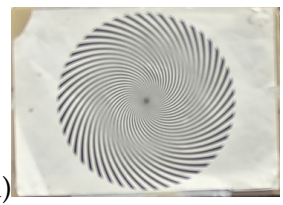 b) 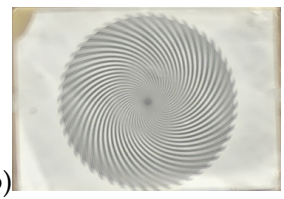

FIGURE 8.37: Zoomed in images of the center Siemens star at a) 0 V on all the piezoelectric stacks, and b) 150V on all the stacks. Note the worsening of the quality in the latter image.

a) b)

FIGURE 8.38: Zoomed in images of the left lower corner Siemens star at a) 0 V on all the piezoelectric stacks, and b) 150V on all the stacks. Note the worsening of the quality in the latter image.

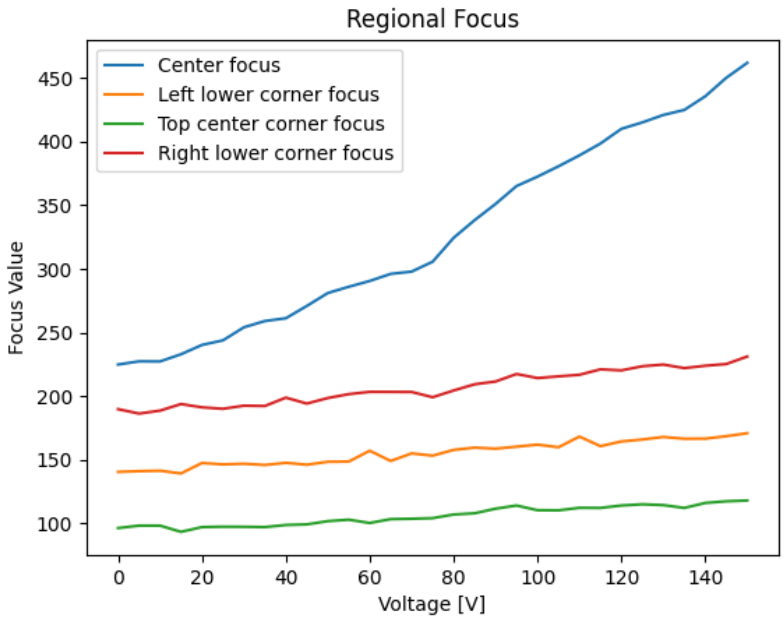

FIGURE 8.39: Graph depicting a bettering in the focus of the image when applying a voltage to the stacks. Note the blue line (Center), having the biggest change of focus.

a)

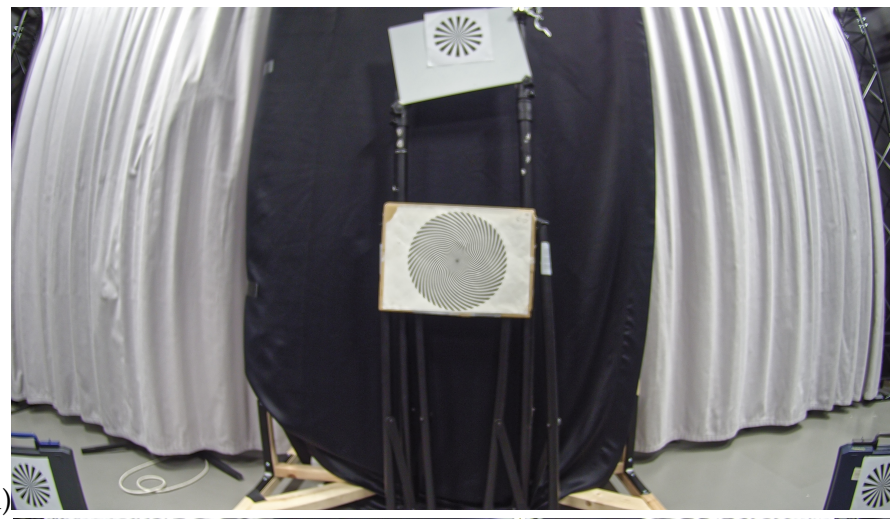

b)

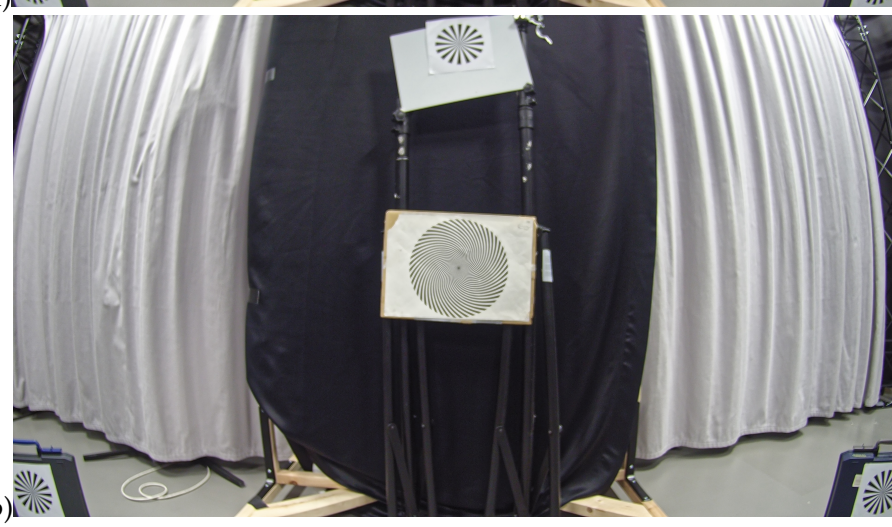

FIGURE 8.40: Images at a) 0 V on all the piezoelectric stacks, and b) 150V on all the stacks. Note the obvious over all improvement of the quality in the latter image.

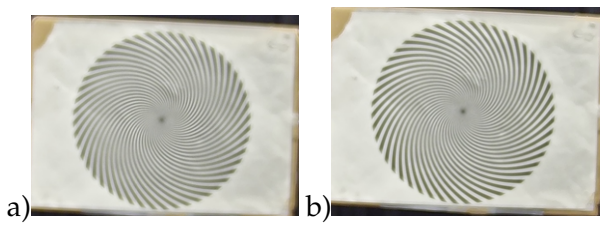

FIGURE 8.41: Images zoomed in at the center Siemens star at a) 0 V on all the piezoelectric stacks, and b) 150V on all the stacks. Note the obvious over all improvement of the quality in the latter image.

In the test in Figure 8.42, a prominent peak is plotted. Being that in the test in this set-up a lens with an f-number of 1.2 was used, a more sensitive response was expected. In the HIT tests when using lenses with f-values of 2.0, a peak could not be plotted with the displacement of 41 μm.

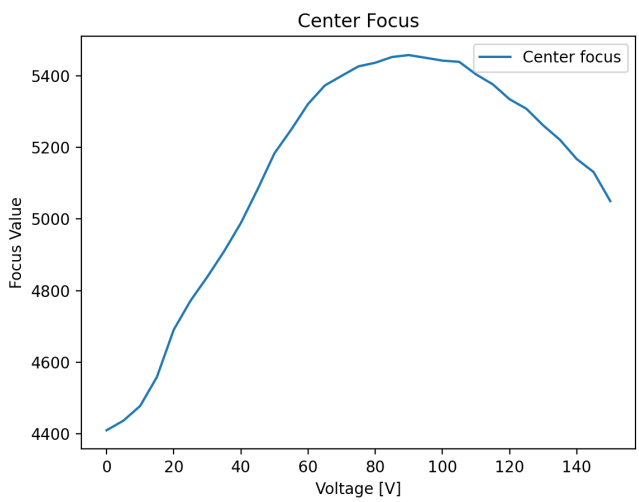

FIGURE 8.42: The Center focus values from the test in Figure 8.43. This specific test shows the focus value peak.

8.3.3 Automatic alignment

In the "Automatic Alignment" tests, the auto focus algorithm in Appendix A was put to test. The idea was that when iterating through the voltages 0-150 V with steps of 5 V, images and the focus values are saved. When the iteration is complete, the controllers are put to the voltage where the center focus value is the best. The code then checks for the worst corner focus value, and then goes through the same iteration, this time only for the corner with the worst value. When the search for the best value is done, the voltage for that value is set for the corner and the algorithm is complete. The Table 8.1 is values from the same test as Figure 8.39, but the starting value, best center value and the values after the worst corner was improved. The same goes for Figure 8.43 and Table 8.2 and Figure 8.44 and Table 8.3.

The large variety in focus value in the different corners and center is dependent on many things for example the sensitivity of the algorithm, the alignment of the sensor in relation to the lens and the difference in the target ROIs from the scene. It can therefore be a bit misleading to compare the exact values to each other and one should rather emphasize on the relative difference within each graph.

TABLE 8.1: Focus values and ratios when running the focus algorithm on the prototype from the test in Figure 8.39.

	Unaltered image	Best Center	Best Center + Corner
Center Corner value	73.8	90.4	94.2
Left Corner value	133.5	154.3	159.5
Right Corner value	172.7	211.4	216.7
Center value	231.3	479.2	531.1
Center Corner ratio	0.3188	0.1888	0.1773
Left Corner ratio	0.5773	0.3220	0.3003
Right Corner ratio	0.7469	0.4412	0.4082
Bottom Corners ratio	0.6621	0.3816	0.3543
Mean of all Corners ratio	0.5477	0.3173	0.2953

By studying Table 8.1 one can see that all separate values, such as center corner value, left corner value, right corner value and center value, improves from the starting value, to the best center value and then further to the best center and alternated worst corner. However, looking at the ratio values a general decreasing trend can be found. This is due to that the center value preform a larger increase in value than the corners. If this is compared to the Figure 8.39 one can see it make sense as the center has, by far, a larger increase in focus value than the corners. The worst corner can also be spotted in Figure 8.39 and was the top center corner. As previously said does the value increase after the algorithm is run.

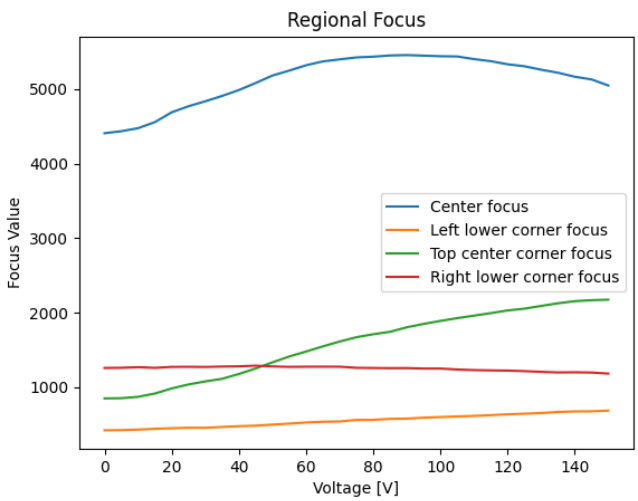

FIGURE 8.43: The focus-graphs for different regions when running the focus algorithm. Note the large difference for the different regions. The corresponding values can be found in Table 8.2.

TABLE 8.2: Focus values and ratios when running the focus algorithm on the prototype from the test in Figure 8.43.

	Unaltered image	Best Center	Best Center + Corner
Center Corner value	631.4	1475.7	1599.7
Left Corner value	351.9	513.5	531.0
Right Corner value	1042.4	1000.8	998.7
Center value	4599.3	5551.6	5442.9
Center Corner ratio	0.1372	0.2658	0.2939
Left Corner ratio	0.0765	0.09250	0.0975
Right Corner ratio	0.2266	0.18027	0.18348
Bottom Corners ratio	0.1516	0.1364	0.1405
Mean of all Corners ratio	0.1468	0.1795	0.1917

It is possible to see a peak of the center value in Figure 8.44. The worse corner is the left lower corner. It is therefore not surprising when the Table 8.3 show how the center value was increased between the staring unaltered image and the best center image, but decreased to the best center and improvement of the worst corner, as the best value for the left corner was at maximum voltage. The top center value also seems to benefit from a higher voltage and is improved when the value after the improvement of the worst corner is done. However, the right lower corner is best at the unaltered image as can be suspected from Figure 8.44.

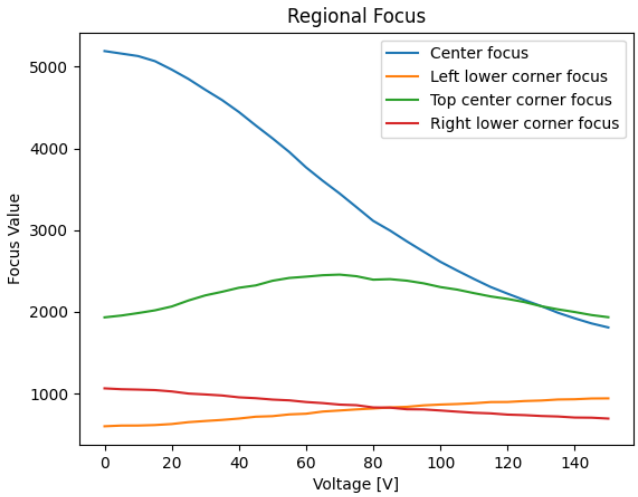

FIGURE 8.44: The focus-graphs for different regions when running the focus algorithm. Note the large difference for the different regions. The corresponding values can be found in Table 8.3.

TABLE 8.3: Focus values and ratios when running the focus algorithm on the prototype from the test in Figure 8.44.

	Unaltered image	Best Center	Best Center + Corner
Center Corner value	1414.9	1482.6	1448.8
Left Corner value	485.2	498.8	725.5
Right Corner value	877.7	866.8	674.5
Center value	5404.2	5295.5	2217.1
Center Corner ratio	0.2618	0.2799	0.6534
Left Corner ratio	0.0897	0.0941	0.3272
Right Corner ratio	0.1624	0.1636	0.3042
Bottom Corners ratio	0.1261	0.1289	0.3157
Mean of all Corners ratio	0.1713	0.1792	0.4283

In Figure 8.44 the center value has the largest amount of relative change in focus value and has a best value at 0 V. The worst corner at low voltages is left lower corner. When the best center value and improving the worst corner is run one can see in Table 8.3 that the left corner value has improved the most, while the center value has drastically decreased. However, the mean value of all corner ratio has greatly increased suggesting an improvement of the over all tilt of the image.

8.3.4 Deliberate tilting

When one deliberately tilts the sensor in relation to the lens, as in Figure 6.16, it is often to achieve a shift in focus so that the image is focused on something else; For example on an object or person further away in a long hallway. In the following test this was done in a controlled environment in an Axis photo studio. The results are compiled in Table 8.4.

TABLE 8.4: Focus values and ratios when deliberately tilting the sensor. Note the bottom and and top ratios.

	Straight	Backtilt	Fronttilt
Center Corner value	743.8	461.3	1685.0
Left Corner value	840.7	810.6	828.3
Right Corner value	347.1	337.9	430.6
Center value	839.8	676.5	1876.0
Center Corner ratio	0.8857	0.6819	0.8981
Left Corner ratio	1.001	1.1982	0.4415
Right Corner ratio	0.4133	0.4995	0.2296
Bottom Corners ratio	0.7072	0.8488	0.3355
Mean of all Corners ratio	0.7667	0.7932	0.5231

If one compares the values of the bottom corner ratio and center corner ratio it is possible to see how the two values changes opposite to each other. In the order of backtilt, straight and fronttilt the center corner ratio changes 0.68188, 0.8857 and 0.89817 and becomes larger. The bottom corner ratio on the other hand goes from 0.84883, 0.7072 to 0.33552 and becomes smaller. This indicates that the two different

parts of the sensor moves in opposite direction, as desired. Compared to the focus graphs, this would mean the bottom corners would move in one direction on the graph and the top center in the other direction. This implies that the sensor is tilting. It however not completely certain as if the sensor moved parallel to the lens and the top center corner and bottom corner focus values are on the opposite sides of respective peak.

At a closer look it is also possible to see that top center corner value follow the trends of the mention ratios. However, the left corner value has largest value (840.699) at the straight position and the right corner vale (430.6) at fronttilt. This could imply that the curves are at different starting positions in respective focus graph. As the change is relatively low it could mean the left corner is close to its focus plateau. It could also suggest that the left piezoelectric stack is not working properly, however, compared to the tables 8.1 to 8.3, which do show a large change in focus, this is very unlikely.

By comparing center values backtilt, straight and fronttilt 676.5, 839.8 and 1876.07 it is possible to see the that the value changes and the center of the sensor is not fixed. This is due to the fact that the point of rotation is not fixed and the entire sensor moves when one stack is extended, as discussed in Chapter 6.4 and Figure 6.19.

8.4 Electrical Measurements

8.4.1 Power Consumption

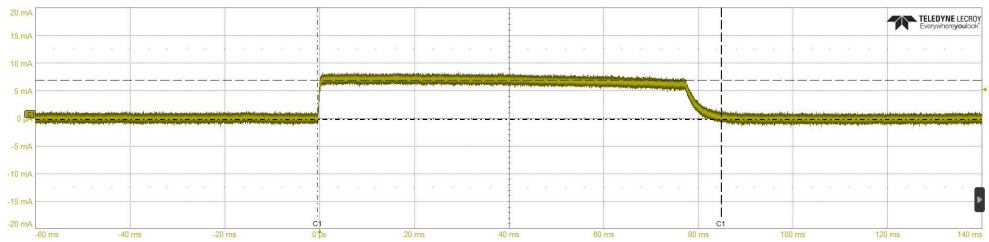

FIGURE 8.45: A screenshot of oscilloscope measurements of the current is shown, captured at the moment when the controller connected to a piezoelectric stack is turned on. The y-axis depicts the current and the x-axis the time. The figure depicts the stack charging up and acting as a capacitive interrupt after the charging process. Note that the current peak lasts for 85-90 ms.

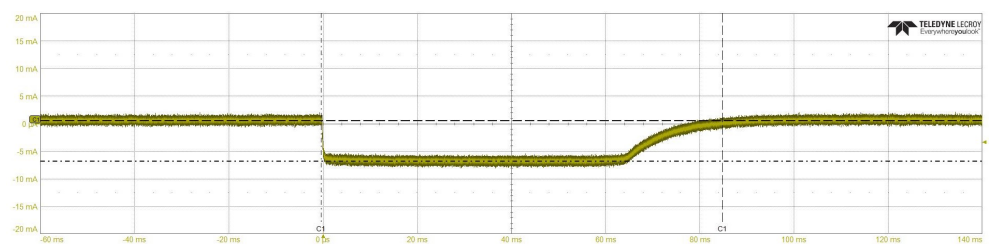

FIGURE 8.46: A screenshot of oscilloscope measurements of the current is shown, captured at the moment when the controller connected to a piezoelectric stack is turned on. The y-axis depicts the current and the x-axis the time. The figure depicts the stack discharging and acting as a capacitive short circuit after the discharging process. Note that the negative current peak lasts for 85-90 ms

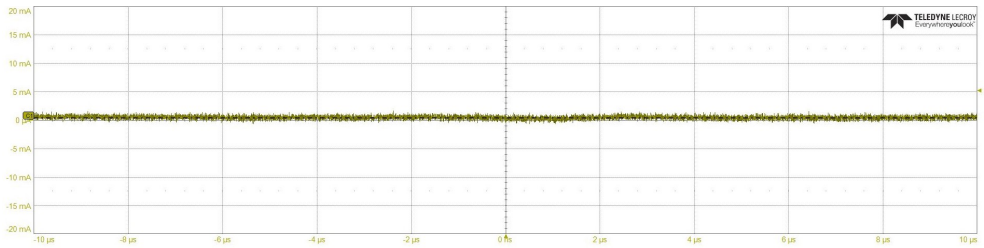

FIGURE 8.47: A screenshot of oscilloscope measurements of the current is shown, captured when the controller is turned off and no current, except for a slight offset of 400 μm, is running through the circuit. The y-axis depicts the current and the x-axis the time.

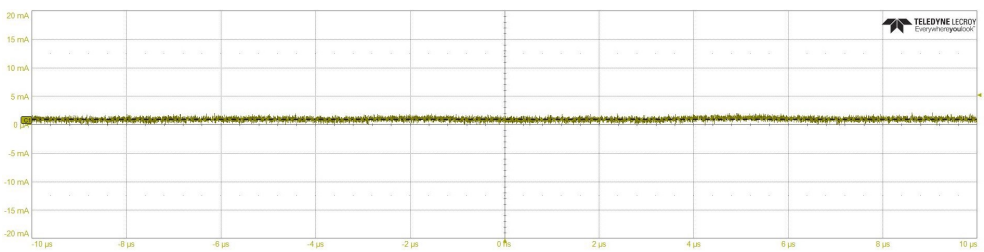

FIGURE 8.48: A screenshot of oscilloscope measurements of the current is shown, captured when the controller has been turned on at 150V for a while. Note the current of 950 μm running through the circuit. The y-axis depicts the current and the x-axis the time.

TABLE 8.5: Oscilloscope measurements of current figures 8.47 and 8.48.

Voltage [V]	Current [A]
0V at t $\approx \infty$	400 μA
150V at t $\approx \infty$	950 μA
0V - 150V at t $\approx$ 0	7.05 mA
150V - 0V at t $\approx$0	-7.4 mA

Figures 8.45 - Figure 8.45 are images using an oscilloscope and a current probe as a stack was charged and discharged. By using equation 2.7, one can calculate the power consumption of each piezoelectric stack when setting the voltage from 0V-150V to be around 1.11W, as seen in Table 8.5 and Figure 8.45, thus the total power consumption is 3.33W but only for 80ms. Depending on what current one supply the stacks with, both the charging time of the stack change and also the power consumption. The Thorlabs-supplied controllers designed for driving the stacks were engineered to maintain a stable current supply of 7.5 mA. The long term power consumption is calculated by using the same equation 2.7 but for the current at t $\approx \infty$ once again from Table 8.5. As seen in Figure 8.47, there is a slight offset at around 400 μA. This means that the current drawn at t $\approx \infty$ is 950 - 400 = 550 μA, thus a power consumption of 82.5 mW each and a total of 247 mW for the majority of the time.

The theoretical and expected current when all three piezoelectric stacks are fully charged at 150 V is approximately 150 μA $\cdot$ 3 = 450 μA, see Equation 5.2. 550 μA seams like a reasonable value as it is close to 450 μA. There might be some margin of error of the accuracy of the resistors used which may affect the result. As well as the signal was quite noisy and where on the graph the measurement should be taken is taken by hand.

The theoretical time it should take to charge and discharge the individual stacks by 99% is 16 ms, if the capacitance is 3500 nF and the stack is in series with a resistance of 1 kΩ, see Equation 2.4 and Equation 2.5. However, the limiting current of 7.5 mA provided by the piezoelectric controller extends the time.

The M3088 camera has, as seen in Table 4.3, a POE class 2 and can be supplied with 3.6-4.2 W. Depending on how much the camera already draws, the initial power consumption of the piezoelectric stacks (3.33 W) could be a problem, but only for 80ms. This could pass if you distribute the power bearing processes, making the stacks charge only when the power consumption of the other parts of the device is as its lowest. Being that the long term power consumption of the three stacks is only 247 mW, this could be a convenient solution if changing to a higher POE class is out of the question. It is possible to lower

the power consumption by supplying the stacks with a lower current. However this will make the charging of the piezoelectric stacks to be slower. Thus making the auto focus algorithm slower in the sense that every time the voltage is increased/decreased, the system would have to "wait" for the stacks before acquiring a focus value for it to be accurate.

Chapter 9

Conclusion & Future Directions

To summarise, the study investigated the most suitable piezoelectric device for precisely aligning the image sensor in Axis Communication cameras. Based on market analysis, a piezoelectric stack was identified as the most appropriate stack. A 3D printed prototype was developed surrounding the company's M-line dome cameras, and tested with a Python-based auto focus algorithm in various environments. Results showed that attaching three piezoelectric stacks with a displacement of 41 μm behind the image sensor of an M3088 Axis dome camera, and adjusting its position relative to the lens, resulted in a noticeable shift in focus. These findings have practical implications for achieving precise alignment in camera systems.

In hindsight, there is a lot of aspects that could have been done differently in order to further prove the significance of the possibilities associated with this technology. A few examples include the choice of camera/cameras, the design of the prototype in order to maximize the amount of tilting that is possible and the displacement of the stacks. These aspects are discussed below.

9.1 The Prototype and The (In)ability to Tilt

When constructing the prototype, a lot more things should have been known and researched. Tilting of the image sensor in relation to the

lens is essential, not only for a successful alignment of the focus-plane, but also when it comes to deliberate tilting; In a long hallway for example, one would want the option of looking further away and something close at the same time and would do so by tilting the sensor along the horizontal axis. In this prototype this was not entirely achievable. In 6.4 "Tilt", the possible tilting angle is discussed, and this was not enough for it to be visible for the naked eye. By constructing the prototype differently one could reach a higher angle for tilting; A larger displacement of the piezoelectric stacks or placing them in a smaller triangle directly under the image sensor. This not only ensures a higher angle for tilting, but also makes it easier to calculate which piezoelectric stack(s) to move in order to achieve the desired focus in each of the regions of the image. However, a steeper tilt would put a larger stress on the stack. One way to avoid this would be to use piezoelectric stack with an end hemisphere. On the other hand this would make the prototype more complicated as this would introduce instability, which would need to be taken into consideration. Overall the prototype constructed was successful in performing simpler focusing by moving the image board in a level position.

9.2 The Cameras

Being that there was, to begin with, limited knowledge about the sensitivities regarding a small shift in focus in the different cameras Axis provide, the only criteria was that the camera (lens and image sensor PCB) was compact and easy to manipulate into a prototype. If this was the right way of going about, is hard to entirely justify. The advantages of this way of choosing camera was that a prototype rather quickly came to realization. If the project was to be revisited, a more detailed investigation of what camera is the most suitable, would be a more prominent aspect in the deciding of what camera(s) to continue on with.

9.3 The Algorithm

To make sure the piezoelectric controllers are supplying the stacks with the right voltage when taking the picture, the controllers are put

to sleep for 5 seconds, as seen in the code in Appendix A. This makes the algorithm slow which is not ideal. If this was not done, the system would be taking an image before the stacks have the correct position, thus given us incorrect values of the focus. Even though the decay time for the stacks are around 80 μm, the timing is limited by the controllers ability to register the input from the code and setting that voltage to the piezoelectric stack. This aspect may be reduced when the power supply is directly integrated in a product.

9.4 Lead Free Piezoelectric Crystals

In the beginning part of the project, a rather comprehensive market study was carried out. Being that the scope of this project only consisted of the testing of the actual principle of moving the image sensor with the piezoelectric phenomenon in relation to the image lens; What composition the crystal had mattered little. Most importantly was the ease of implementation, a large displacement without being to large, small cost and a fast shipping time. All this came in the package of the PZT piezoelectric stack, the downside being that the package was wrapped up in a film of lead.

There is an interest in developing lead-free piezoelectric material, due to the potential environmental pollution. Multiple different scholars have begun to study potential suitable materials. At this time the most promising material is a perovskite but with lead free compositions. However, when these materials are compared to the market-leading piezoelectric material such as PZT, they show low stability and sensitivity to high temperature. A smaller displacement and their high price tag also calls for a moment of concern. Another alternative is a material with a completely different composition: Potassium Sodium Niobate (KNN). It has a large piezoelectric constant and other characteristics as great as PZT [16]. As of now KNN is not used as the sole material in a piezoelectric component, but is used to dilute the amount of PZT used. Examples on these kinds of devices are created by the company TANiOBIS [21] for example.

It is of importance to Axis to consider lead free alternatives if the implementation of piezoelectric devices becomes of interest. One can not

predict when a shift in the regulations might occur. As of now, PZT is exempted from the lead regulations due to the fact that banning its existence in components like this, would cause a big disruption to the industry. However, the damage caused to the environment is a far greater disruption if lead continues to be in use. The more products containing lead that is manufactured, the more lead will need to be disposed of in a responsible way.

9.5 The Type Of Piezoelectric Device

In this pilot study, majority of the focus was placed on the technology: Is it possible to place a piezoelectric crystal behind an image sensor in order to align its position in relation to the optics? Whether this was done using stacks, motors or other compositions of a piezoelectric device mattered little. Given additional time, money, and resources, it is worth considering whether simple piezoelectric stacks would still be the preferred option. The benefits of using other devices are great. The use of self locking piezoelectric devices means not having to constantly power the devices if the placement of the sensor gives the desired focus and could save a lot of energy. Other piezoelectric motors have a far greater displacement than 41 μm while still remaining relatively small, this means that one does not have to rely on the fact that the sensor already is placed with a good enough precision. If the piezoelectric device behind the image sensor could compensate for all the error made in production when assembling the camera, Axis could potentially make the production faster, thus all the alignment is made on site using a micro meter precise stacks along with a focus algorithm built in to the system, instead. The possibilities are endless with this technology, and by conducting this study with simpler stacks and still managing to achieve good results only proves that this, in fact, could benefit Axis, whether they choose to proceed with stacks or other piezoelectric devices.

9.6 Power Consumption

Being that the power consumption is, for most of the time negligible, this technology is very implementable in an Axis product. However,

in this thesis, the way of supplying the stacks with power was using separate controllers. In a product this, of course, is not feasible. Being that most piezoelectric devices uses a high voltage, there is a need to drive a voltage on the main PCB to 150V, in this case. This could be done by integrating a high-voltage step-up converter or a specialized power supply module into the device. An option for this would be the "Industrial piezo driver with integrated 105-V boost converter" [10].

9.7 Products in Need of This Technology

If the idea of using piezoelectric stacks would be explored further, what would be what kind of camera that would benefit the most from this technique? If a camera has consistent problems with misalignment it might be beneficial to use stacks as a solution. An example could be a camera which is exposed to large alternating temperature changes, where the material in the camera could move and create problems, or cameras with extremely high resolution that are inherently sensitive to shifts in focus. Piezoelectric stack could be targeted towards cameras with these kinds of problems.

As the piezoelectric stacks have an extremely high precision of micrometer (or even nanometer) it could be beneficial to cameras with very high sensitivity. Even if a camera have the possibility to adjust focus it is most common done by adjusting and moving the lens of the camera. By using piezoelectric stacks a movement of the sensor could be used in combination with already existing focusing method as a way to create a broader range of focus and also adjust the focus with more precision with the use of tilting. The unique function to be able to tilt the sensor would be very beneficial to all cameras but especially those which are the most sensitive, where unwanted tilt of the sensor would create large problems. Even though this prototype could not explicitly prove the ability to tilt, theory strongly suggest it would succeed if reconstructed.

Voluntary tilt could also be used as a way to have a shifted focus plane, where one part of the sensor could have a closer focus and the other part a more distant focus. This could be used in for example malls,

office spaces and long streets where objects are placed both close and far away from the camera.

Another idea could be to use three piezoelectric stacks as a fine tuning mechanism in combination with a rougher set-up that would move the sensor board in relation to the lens and the piezoelectric stacks would only adjust the tilt. This way the piezoelectric stack would be shorter and the price, as well as amount of lead used could be lowered, if Axis chooses to go the PZT route.

Appendix A

Auto Focus Algorithm

.1 Class Camera

```
class Camera:
    def __init__(this,ip_nbr):

        this.ip_nbr=ip_nbr
        #169.254.204.10gamla  169.254.241.157 nya
        this.cap = cv2.VideoCapture(f"http://root:
           pass@{this.ip_nbr}/jpg/image.jpg?
           compression=0")
        # check if connection is successful
        if not this.cap.isOpened():

            raise ConnectionError("Could not connect
               to camera")

        else:
            print("Connected to camera")


    def getImage(this,devices,time):
        this.cap = cv2.VideoCapture(f"http://root:
           pass@{this.ip_nbr}/jpg/image.jpg?
           compression=0")
        ret, frame = this.cap.read()
        # check if frame is valid

        if ret:
                # check if frame is valid
```

```
                voltages=[]
                for x in devices:
                    voltages.append(float(str(x.
                        getOutputVoltage()).replace(',
                        ', '.')))

                filename = f"{voltages}"

                    # Convert list to JSON-formatted
                        string
                path=f'C:/Users/reemc/Desktop/
                    projekt2/{time}'

                if not os.path.exists(path):
                    os.makedirs(path)
                cv2.imwrite(f'C:/Users/reemc/Desktop/
                    projekt2/{time}/{filename}.jpg',
                    frame)

                image=frame
                return frame
        else:
            print("Could not take a picture")

    def getCornerFocusValue(this,image,nbr):

         # Convert the image to grayscale
        gray = cv2.cvtColor(image, cv2.COLOR_BGR2GRAY
            )

        height, width = gray.shape

        # Define the regions of interest (ROI) for
            the corners
        marginal=110

        if nbr==0:

            point = (marginal, height-marginal)
        if nbr==1:
            point = (int(width/2), marginal)
        if nbr==2:
            point = (width-marginal, height-marginal)
```

```
        x, y = point

        roi = gray[y-marginal:y+marginal, x-marginal:
            x+marginal]
        corner_value=cv2.Laplacian(roi, cv2.CV_64F).
            var()

        # Draw a rectangle around the current ROI
            corner
        cv2.rectangle(image, (x-marginal, y-marginal)
            , (x+marginal, y+marginal), (0, 255, 0),
            2)

        path=f'C:/Users/reemc/Desktop/projekt2/ROI'

        if not os.path.exists(path):
            os.makedirs(path)

        cv2.imwrite(f'C:/Users/reemc/Desktop/projekt2
            /ROI/{nbr}.jpg', image)


        return corner_value

    def getCenterFocusValue(this,image):

            # Convert the image to grayscale
        gray = cv2.cvtColor(image, cv2.COLOR_BGR2GRAY
            )

        marginal=240

        # Define the region of interest (ROI) for the
            center point
        height, width = gray.shape
        roi_center = (int(width/2), int(height/2))
        # Define the regions of interest (ROI) for
            the corners

        center_value = cv2.Laplacian(gray[roi_center
            [1]-marginal:roi_center[1]+marginal,
```

```
                                        roi_center
                                            [0]-
                                            marginal:
                                            roi_center
                                            [0]+
                                            marginal],
                                             cv2.
                                            CV_64F).
                                            var()

        x, y = roi_center
         # Draw a rectangle around the current ROI
             corner
        cv2.rectangle(image, (x-marginal, y-marginal)
            , (x+marginal, y+marginal), (0, 255, 0),
            2)

        path=f'C:/Users/reemc/Desktop/projekt2/ROI'

        if not os.path.exists(path):
            os.makedirs(path)

        cv2.imwrite(f'C:/Users/reemc/Desktop/projekt2
            /ROI/center.jpg', image)

        return center_value
```

.2 Class Device

```
clr.AddReference('C:\\Program Files\\Thorlabs\\
    Kinesis\\Thorlabs.MotionControl.DeviceManagerCLI.
    dll')
clr.AddReference('C:\\Program Files\\Thorlabs\\
    Kinesis\\Thorlabs.MotionControl.GenericMotorCLI.
    dll')
clr.AddReference('C:\\Program Files\\Thorlabs\\
    Kinesis\\ThorLabs.MotionControl.KCube.PiezoCLI.dll
    ')
from Thorlabs.MotionControl.DeviceManagerCLI import *
from Thorlabs.MotionControl.GenericMotorCLI import *
```

```
from Thorlabs.MotionControl.KCube.PiezoCLI import *
from System import Decimal  # necessary for real
    world units
from datetime import datetime


class Device:

    def __init__(this, serial_no, nbr):

        this.serial_no=serial_no
        this.nbr=nbr

        DeviceManagerCLI.BuildDeviceList()
        devices = DeviceManagerCLI.GetDeviceList(
            KCubePiezo.DevicePrefix)

        # Connect, begin polling, and enable
        this.device=KCubePiezo.CreateKCubePiezo(
            serial_no)
        this.device.Connect(serial_no)
        # Start polling and enable
        this.device.StartPolling(250)  #250ms polling
             rate
        time.sleep(1)
        this.device.EnableDevice()
        time.sleep(0.25)  # Wait for device to enable

        if not this.device.IsSettingsInitialized():
            this.device.WaitForSettingsInitialized
                (10000)  # 10 second timeout
            assert this.device.IsSettingsInitialized
                () is True

        # Set the Zero point of the device
        this.device.SetMaxOutputVoltage(Decimal(150))

        print('Setting device: '+ str(nbr) +' to Zero
             Point')
        this.device.SetZero()

    def getnbr(this):
        return this.nbr
```

```
    def disconnectDevice(this):
        this.device.SetZero()
        time.sleep(3)
        print(f'Moved to Voltage {this.device.
            GetOutputVoltage()}')
        # Stop Polling and Disconnect
        this.device.DisableDevice()
        this.device.StopPolling()
        this.device.Disconnect()

    def setVoltage(this,voltage):

        # Get the maximum voltage output of the KPZ
        max_voltage = this.device.GetMaxOutputVoltage
            ()  # This is stored as a .NET decimal

        # Go to a voltage
        dev_voltage = Decimal(voltage)
        print(f'Going to voltage {dev_voltage}')

        if dev_voltage >= Decimal(0) and dev_voltage
            <= max_voltage:
             this.device.SetOutputVoltage(dev_voltage)
            # time.sleep(1)
        else:
             print(f'Voltage must be between 0 and {
                max_voltage}. Your input was {
                dev_voltage}')

    def getOutputVoltage(this):

        return this.device.GetOutputVoltage()
```

.3 Main

```
if __name__ == '__main__':
    try:
        now = datetime.now()
```

```
date_string = now.strftime("%Y-%m-%d")
time_string = now.strftime("%H-%M-%S")
times = f"{date_string}{time_string}"

camera=Camera("169.254.241.157")
device0=Device("29252447",0)
device1=Device("29252477",1)
device2=Device("29252353",2)

devices=[device0,device1,device2]

voltages = list(range(0, 151, 5))

centerFocus={
}
device0_cornerfocus={}
device1_cornerfocus={}
device2_cornerfocus={}

image=camera.getImage(devices,times)

for v in voltages:
    device0.setVoltage(v)
    device1.setVoltage(v)
    device2.setVoltage(v)
    time.sleep(5)
    image=camera.getImage(devices,times)

    centerFocus.update({v: camera.
        getCenterFocusValue(image)})
    device0_cornerfocus.update({v: camera.
        getCornerFocusValue(image,0)})
    device1_cornerfocus.update({v: camera.
        getCornerFocusValue(image,1)})
    device2_cornerfocus.update({v: camera.
        getCornerFocusValue(image,2)})

max_centerFocus=max(centerFocus.items(),key=
    lambda x:x[1])

print(centerFocus)
print(max_centerFocus)
```

```
device0.setVoltage(max_centerFocus[0])
device1.setVoltage(max_centerFocus[0])
device2.setVoltage(max_centerFocus[0])
time.sleep(5)
image=camera.getImage(devices,times)

device0_corner = {device0: camera.
   getCornerFocusValue(image, device0.getnbr
   ())}
device1_corner = {device1: camera.
   getCornerFocusValue(image, device1.getnbr
   ())}
device2_corner = {device2: camera.
   getCornerFocusValue(image, device2.getnbr
   ())}

list_of_devices_and_corners=[device0_corner,
   device1_corner,device2_corner]

worst_corner_value = float('inf')
worst_corner_device = None

for device_corner_dict in
   list_of_devices_and_corners:
    for device, corner in device_corner_dict.
       items():
        if corner < worst_corner_value:
            worst_corner_value = corner
            worst_corner_device = device

print("the worst corner value: " + str(
   worst_corner_value))
print("the worst corner device: "+ str(
   worst_corner_device.getnbr()))

voltages_corner=list(range(0, 151, 5))

cornerFocus={
}
for v in voltages_corner:
    time.sleep(5)
    image=camera.getImage( devices,times)
    worst_corner_device.setVoltage(v)
```

```
    cornerFocus.update({v: camera.
        getCornerFocusValue(image,
        worst_corner_device.getnbr())})

max_cornerFocus_voltage = max(cornerFocus,
    key=lambda x: cornerFocus[x])

worst_corner_device.setVoltage(
    max_cornerFocus_voltage)
time.sleep(5)
image=camera.getImage(devices,times)

print("The new center focus value: "+str(
    camera.getCenterFocusValue(image))+" the
    previous: "+  str(max_centerFocus))
print("The new corner focus value for device0
    : "+str(camera.getCornerFocusValue(image,
    device0.getnbr()))+" the previous: "+ str(
    list(device0_corner.values())[0]))
print("The new corner focus value for device1
    : "+str(camera.getCornerFocusValue(image,
    device1.getnbr()))+" the previous: "+ str(
    list(device1_corner.values())[0]))
print("The new corner focus value for device2
    : "+str(camera.getCornerFocusValue(image,
    device2.getnbr()))+" the previous: "+ str(
    list(device2_corner.values())[0]))
time.sleep(5)

device0_cornerfocus_final=camera.
    getCornerFocusValue(image,0)
device1_cornerfocus_final=camera.
    getCornerFocusValue(image,1)
device2_cornerfocus_final= camera.
    getCornerFocusValue(image,2)
centerFocus_final=camera.getCenterFocusValue(
    image)

device0.disconnectDevice()
device1.disconnectDevice()
device2.disconnectDevice()

Values = {
```

```
'Date & Time' : times,
'Center focus value': centerFocus,
'Device 0 Corners focus values':
   device0_cornerfocus,
'Device 1 Corners focus values':
   device1_cornerfocus,
'Device 2 Corners focus values':
   device2_cornerfocus,
'END VALUE0': device0_cornerfocus_final ,
'END VALUE1': device1_cornerfocus_final,
'END VALUE2': device2_cornerfocus_final,
'END VALUECenter':centerFocus_final,
'Voltages' : voltages
}

  # Convert list to JSON-formatted string
path=f'C:/Users/reemc/Desktop/projekt2/{times
   }'

if not os.path.exists(path):
    os.makedirs(path)

file_path = f'C:/Users/reemc/Desktop/projekt2
   /{times}/values.txt'
json_string = json.dumps(Values)

 # Write JSON string to text file
with open(file_path, 'a+') as f:
    f.write(json_string)

plt.figure()
# Plot test 1
plt.plot(voltages, centerFocus.values(),
   label='Center focus')
plt.plot(voltages, device0_cornerfocus.values
   (), label='Left lower corner focus')
plt.plot(voltages, device1_cornerfocus.values
   (), label='Top center corner focus')
plt.plot(voltages, device2_cornerfocus.values
   (), label='Right lower corner focus')

# Add a title and labels to the graph
plt.title('Regional Focus')
```

```
        plt.xlabel('Voltage [V]')
        plt.ylabel('Focus Value')

        # Add a legend to differentiate the vectors
        plt.legend()
        plt.savefig(f'C:/Users/reemc/Desktop/projekt2
            /{times}/Focus_Values.png')

        plt.show()

    except Exception as e:
        print("Something went wrong: "+ str(e) + " .
            Disabling the devices.")
        device0.disconnectDevice()
        device1.disconnectDevice()
        device2.disconnectDevice()
```

Bibliography

[1] Axis Communications AB. Om axis communications. https://www.axis.com/sv-se/about-axis. Accessed: May 13, 2023.

[2] Axis Communications AB. Ten reasons to switch to ip-based video. https://www.axis.com/learning/web-articles/ten-reasons-to-switch-to-ip-based-video/crystal-clear-motion, note=Accessed: May 13, 2023.

[3] Axis Communications AB. Ccd and cmos sensor technology technical white paper. https://www.axis.com/files/whitepaper/wp_ccd_cmos_40722_en_1010_lo.pdf, 2010. Accessed: May 13, 2023.

[4] Axis Communications AB. Axis m3065-v dome camera specifications. https://www.axis.com/dam/public/b5/47/cd/datasheet-axis-m3065-v-network-camera-en-US-378348.pdf, 2020. Accessed: May 12, 2023.

[5] Axis Communications AB. Axis m3088-v dome camera specifications. https://www.axis.com/dam/public/79/89/e2/datasheet-axis-m3088-v-dome-camera-en-US-388266.pdf, 2022. Accessed: May 13, 2023.

[6] Raghav Bansal, Gaurav Raj, and Tanupriya Choudhury. Blur image detection using laplacian operator and open-cv. pages 63–67, 2016.

[7] PI Ceramic. Piezo technology. https://www.piceramic.com/en/expertise/piezo-technology, 2023.

[8] Mats Gustafsson Daniel Sjöberg. Kretsteori, ellära och elektronik. pages 17–126, 2018.

[9] Guangya Ding, Zijun Xing, Naiyu Chen, Jun Wang, and Li Shi. Fatigue behaviour of piezoelectric ceramic stack under large cyclic dynamic loading. https://doi.org/10.1177/1045389X221147672, 2023. Accessed: May 13, 2023.

[10] Texas Instruments. Drv2700 industrial piezo driver with integrated boost converter. https://www.ti.com/product/DRV2700#tech-docs, 2023. Accessed: May 15, 2023.

[11] Haonan Jin, Xiangyu Gao, Kaile Ren, Jinfeng Liu, Liao Qiao, Mingzi Liu, Wei Chen, Yuhang He, Shuxiang Dong, Zhuo Xu, and Fei Li. Review on piezoelectric actuators based on high-performance piezoelectric materials. *IEEE Transactions on Ultrasonics, Ferroelectrics, and Frequency Control*, PP, 05 2022.

[12] Tae-Hwan Kim. An efficient barrel distortion correction processor for bayer pattern images. *IEEE Access*, 6:28239–28248, 2018.

[13] Y. Sakabe M. Kimura, A. Ando. Lead zirconate titanate-based piezo-ceramics. https://www.sciencedirect.com/science/article/pii/B9781845695347500029, 2010. Accessed: May 13, 2023.

[14] Markforged. Micro carbon fiber filled nylon that forms the foundation of markforged composite parts. https://markforged.com/materials/plastics/onyx. Accessed: May 14, 2023.

[15] European Parliment. Directive 2011/65/eu of the european parliament and of the council of 8 june 2011 on the restriction of the use of certain hazardous substances in electrical and electronic equipment (recast) text with eea relevance. https://eur-lex.europa.eu/eli/dir/2011/65/oj, 06 2011. Accessed: May 16, 2023.

[16] Mark A. Rambaran. Tunable surfaces using polyoxoniobates and -tantalates as molecular building blocks. https://www.diva-portal.org/smash/get/diva2:1690097/FULLTEXT01.pdf, 2022.

[17] Reac-group. What is an actuator? https://www.reac-group.com/en_en/facts/actuators/what-is-an-actuator/, 2023. Accessed: May 09, 2023.

[18] P. K. Sinha. Image acquisition and preprocessing for machine vision systems. 2015.

[19] G. Smith. Ocular defocus, spurious resolution and contrast reversal. https://onlinelibrary.wiley.com/doi/abs/10.1111/j.1475-1313.1982.tb00159.x, 1982. Accessed: May 13, 2023.

[20] Warren J. SMith. Modern optical engineering : the design of optical systems 4th edition. pages 10–387, 2008.

[21] Taniobis. https://www.taniobis.com/technology-innovation/materials-for-green-technology.a3.en.html. Accessed: May 09, 2023.

[22] Thorlabs. Kch301 - usb controller hub and power supply for three k-cubes or t-cubes. https://www.thorlabs.com/thorproduct.cfm?partnumber=KCH301, 2015. Accessed: May 02, 2023.

[23] Thorlabs. Kpz101 - k-cube piezo controller. https://www.thorlabs.com/thorproduct.cfm?partnumber=KPZ101, 2015. Accessed: May 02, 2023.

[24] Thorlabs. Pk4fyp1 - discrete piezo stack, 150 v, 41.0 µm displacement, 5.0 mm x 5.0 mm x 38.1 mm, end hemisphere and flat end plate. https://www.thorlabs.com/thorproduct.cfm?partnumber=PK4FYP1, 06 2015. Accessed: April 25, 2023.

[25] Thorlabs. Apf503 - amplified piezoelectric actuator with flexure mount, 150 v, 390 µm max displacement. https://www.thorlabs.com/thorproduct.cfm?partnumber=APF503, 07 2017. Accessed: May 03, 2023.

[26] Thorlabs. Pk4fyp2 - discrete piezo stack, 150 v, 41.0 µm displacement, 5.0 mm x 5.0 mm x 36.0 mm, two flat end plates. https://www.thorlabs.com/drawings/5ff703b721337498-45CC9A65-984D-7436-317FB8B28F03F58D/PK4FYP2-SpecSheet.pdf, 06 2020.

[27] S. Trolier-McKinstry, Shujun Zhang, Andrew Bell, and Xiaoli Tan. High-performance piezoelectric crystals, ceramics, and films. *Annual Review of Materials Research*, 48, 11 2017.

[28] TrumanMetz. kpz101-pythonnet. https://github.com/Thorlabs/Motion_Control_Examples/blob/main/Python/KCube/KPZ101/kpz101_pythonnet.py, 2023.

[29] Wikipedia. Siemens star — Wikipedia, the free encyclopedia. http://en.wikipedia.org/w/index.php?title=Siemens%20star&oldid=1073597000, 2023. Accessed: May 07, 2023.

[30] Don Williams and Peter D. Burns. Evolution of slanted edge gradient sfr measurement. https://doi.org/10.1117/12.2042706, 2014.